Journal: Natural Hazards and Earth System Sciences (NHESS)
Revised version of: "A hazard model of subfreezing temperatures in the United Kingdom using vine copulas"
Author(s): Symeon Koumoutsaris
MS No.: nhess-2017-389
MS Type: Research article

General comment

I found the paper improved, and I appreciate the effort of the author in addressing the issues about the uncertainty. There are a couple of steps in the procedure employed for computing the uncertainties which are not fully clear to me. These steps might be potentially important. In principle, these steps might substantially affect/increase the computed model uncertainty. After these are addressed, I would suggest considering the paper for publication.
In the following, I will refer to the pages and lines of the pdf file including the corrections (in blue and red). My revision should be read, again, as a constructive advice.

I would like first of all to thank the reviewer for his valuable comments and corrections. In particular, with respect to the uncertainty calculation, indeed I erroneously computed them (by simulating only the uniform variables and fit the RVM to them only as the reviewer has thought so), which severely underestimated the confidence intervals.

After computing the confidence intervals correctly, the resulting uncertainty is quite large, similar to the empirical one. In order to reduce this large uncertainty, I have decided to:

a) Use a longer historical data set (reanalysis data of 110 years instead of 51 years previously)
b) Lower the resolution in order to decrease the dimension of the joint pdf (67 cells instead of 170 previously)

The resulting confidence intervals however are still quite large. Nevertheless, the longer dataset enabled me to include some physical parameters in the model (notably the influence of NAO and of climate change) that I found useful. I reply to the comments one-by-one below.

Comments related to uncertainty quantification

P1 l8-9 "The model suggests that the extreme winter 1962/63 has a return period of approximately once every 89 years, with 95% confidence intervals between 81 to 120 years. However, the relative short record length together with the unclear effects of anthropogenic forcing on the local climate add considerable uncertainty to this estimate."
Given the "However", I am not sure that it is fully clear, here, that the uncertainty (95% CI) is due to the shortness of the data. In principle, the purpose of the uncertainty quantification is to account for the model uncertainty due to the shortness of the data. I see that you write in the following sentence "add considerably uncertainties", which might be related to acknowledging that the employed procedure to compute the model uncertainty does not account for all of the uncertainties due to the short data length. But this sentence might be improved.
I rephrased to make it more clear:
"However, the estimated uncertainty in these results is quite large and comes from the relatively short record length. Moreover, possible spurious trends in the historical data add considerable uncertainty to these estimates, as well."

P11 l13 "Both together result in a virtual reduction in the dimensions of the pdf." As I wrote in my first comment: "The author says that he is using many independent copula: if this is a reasonable choice then it corresponds to somehow virtually reduce the dimension of the pdf ." I would like to observe that I employed the "somehow virtually reduce" expression in the

response, however, I have never seen this used in the literature.
I took out this comment.

P12 l 1. Section 3.1.2. You might consider changing the title of the section, referring to the uncertainties. In fact, this section explains the procedure to compute the uncertainties.
I have renamed the section as "Stochastic simulation and uncertainty estimation via parametric bootstrap".

P12 l2 "The RVM is used to simulate 10K years of winter-seasons in the UK. For each year, the simulated AFI values at each grid cell depend on the other cells based on the fitted RVM."
To guide the reader, I would explain why the model is used to simulate a so long sample. To reduce the uncertainties associated with the simulation (as explained in my previous comment, see the end of this document).

I have increased the simulation period (to 100K) and added the following sentences: "Performing long enough simulations is necessary in order to obtain converged numerically results, i.e. to convergence to the "true" return period. Our focus here is the 200 year RP, which is commonly associated with capital and regulatory requirements. By repeating the simulation several times, it has been assessed that 100K years of winter seasons is long enough and the Monte Carlo simulation error is negligible. "

P12 l6 "Following Bevacqua et al. (2017), the model uncertainty is assessed using a parametric bootstrap approach..."
[Definition for the following discussion: Let's define procedure1 and procedure2 the two procedures you present on page 13.]
Procedure1. While Bevacqua et al. consider the uncertainties of the marginal pdfs during the procedure, it is not clear to me whether these are accounted for here. **Thus, I am wondering if procedure2 is used to compute the uncertainty associated with the RVM only, or the uncertainty of the full model, i.e. of the joint pdf.** Specifically, going through the first 2 steps of procedure1, it is not clear to me whether you (a) simulate the real data (real, i.e. you transform the uniform variables simulated from the vine using the inverse marginal pdfs) and fit again both the marginals and the RVM to these "real" data, or (b) you simulate only the uniform variables and fit the RVM to them only.
If the procedure is (b), then this is different from the cited Bevacqua et al., and then I think that it should be stated (note that also procedure2 is an addition with respect to Bevacqua et al., but this is not clear). Other differences that would need to be highlighted:
- P12 l7 "...data from the selected RVM." in Bevacqua this is "...data from the selected joint pdf".
- Similarly at p13 l1. "In the selected RVM" in Bevacqua this is "...in the selected joint pdf".
- Similarly at p13 l4. "A new RVM is fitted…" in Bevacqua this is "...a new joint pdf is fitted (via vines)...".
Also, if you do not account for the uncertainty of the marginals (i.e. if you follow (b)), then I recommend to not talk about "model uncertainty (e.g., in line 6), but of RVM uncertainty only. However, the following comment is relevant.
The obtained uncertainty associated with the "model" seems very small (as you also argue later (p19 l30)). You might agree with me that this might be unexpected, given the small sample size. Thus, I am wondering if they are the uncertainty associated with the RVM only, or the uncertainty of the full model, i.e. of the joint pdf. Specifically, I am wondering about: (1) how the model uncertainty would actually be affected by the uncertainty of the marginals (if you do not account for this already, i.e. if you follow (b)); (2) how the model uncertainty increases when the RVM structure is not fixed in procedure1 (step2).
Is there any reason for not considering these two uncertainties? (Again, maybe you already accounted for the marginal uncertainty (1)).

I can see that accounting for all of these uncertainties might be cumbersome strictly following procedure1. To my understanding, an easier alternative to procedure1 (to account for all the model uncertainty, i.e. to also account for (1) the marginal uncertainties and (2) the RVM structure uncertainties), you might consider the following: Applying procedure2*, but simulating 51 years of data (instead of 10k years). This alternative procedure should, in fact, give similar results to applying procedure1 (where also (1) the marginal uncertainties and (2) the RVM structure uncertainties are considered). In this case, it is clear that you would obtain larger uncertainties than obtained via the employed procedures (as you would procedeed as done for procedure2 but employing a much shorter sample).**

***Clearly, the "real" data should be simulated, i.e. one should simulate the uniform variables from the vine, and then transform them into "real" variables employing the inverse marginal CDFs.

As mentioned above, indeed I had computed erroneously the confidence intervals. This has been now corrected. More precisely, as explained in the revised manuscript, the confidence intervals are computed now as follows:

- A simulation with the same length as the observed data (i.e. 110 years) is repeated for B = 500 times.
- For each of these B = 500 samples, a new full model is fitted (including new GEV and logistic regression model parameters at each cell and new RVM structure, pair-copula families and parameters) following the methodology described in sections 3.2.1 and 3.3.1.
- For each of the resulting B = 500 RVMs, a simulation of 10K years of winter-seasons is performed. The uniform variables are then transformed using the (new) inverse marginal pdfs and the corresponding return period levels are estimated.
- The uncertainty in the return levels is estimated by identifying the 95% confidence interval (i.e. the range 2.5–97.5 %) from these 500 return level curves.

Due to computational constraints, confidence intervals are computed only for the stationary model and the simulation length has been reduced to 10K years (instead of 100K). In order to separate the uncertainty associated with the RVM only from the uncertainty of the full model, i.e. of the joint pdf, confidence intervals have been also calculated with the same approach described above, but using the same marginal pdfs in each bootstrap repetition.

Furthermore, I would like to note that I have also computed the confidence intervals using the alternative procedure proposed by the reviewer above and indeed I get the similar results to the procedure above (as the reviewer also suggested). This method is less computer intensive however, the resulting confidence intervals only up to 110 year RP (the historical record length) and thus it does not give a complete picture of the (large) uncertainty. In addition, I wanted to separate the uncertainty originating from the RVM only and compare it with the full model uncertainty, which is not possible with this alternative procedure.

Consideration. To my understanding, showing the Monte Carlo uncertainty (procedure2) in the paper helps to see that the RVM uncertainty (procedure1) is almost the same as the Monte Carlo uncertainty, and therefore you can conclude that the RVM uncertainty is negligible. I see the reasoning, and in principle I like it; however, see the previous discussion about the RVM uncertainty which might become larger if computed differently. Otherwise, personally, I have difficulties in seeing a reason for describing and employing procedure2. **Thus, the reader should be helped to understand the differences between the two uncertainty procedures, e.g. explaining why they are both computed.**
I understand the reviewer's point and I have indeed increased the number of simulation years to 100K (instead of 10K) which makes the Monte Carlo uncertainty negligible.

However, some (small) Monte Carlo uncertainty might still be present in the computed confidence intervals since for computational reasons I had to use a shorter simulation period (10K).

P17 l24-25
According to me, a comparison between purely Monte Carlo uncertainties (obtained simulating an as long as possible sample size) and uncertainties of the "empirical curve" is not conceptually meaningful. As stated in the previous comment revision (see the end of this file), the purely Monte Carlo uncertainties (obtained simulating an as long as possible sample size) is meaningful only to quantify the uncertainty driven by the limited length of the simulation (from a given a pdf that might be assumed to be non-biased).
Instead, it makes sense to me to compare the uncertainty computed using procedure1 with the uncertainties of the "empirical curve". (As stated in the previous pages, I see a sense in comparing uncertainties form procedure1 and procedure2 for stating that the RVM uncertainties are negligible. However, I discussed potential issues of procedure2 above).
I agree and I do not compare the two uncertainties anymore.

P17 l26. "The accuracy can be improved by increasing the number of simulated years, but at a computational cost". I am not comfortable with the message that might be taken from this sentence. The purely Monte Carlo uncertainty can be reduced by simulating long samples, but it should be clear that this is not related with the uncertainty of the model (in a general case).
I have deleted this sentence.

Other comments
P3 l25 "(1)"
Please, write "equation (1)" or "eq. (1)".
Corrected

Eq (1):
Write AFI_Year maybe?
Corrected

Should the AFI_Year be defined as =0 if there are no days with negative temperatures? It is currently not exactly defined in this case, while you refer to f(x) for x=0 in equation 3.
Corrected

Figure 2. Not necessary , but you might consider plotting the -NAOI rather than the NAOI (or -mAFI) to highlight the correlation between the time series.
I have changed the plot and I believe it is more clear now

P5 l8 "exceed"? P(X<=x)
Corrected

P6 l15 "in order to geographically smooth the GEV.."
You might explain the reason for wishing to have smoothed parameters.
I have added the following sentence: "The smoothing increases the sample size at each grid point, which thus leads to a more precise estimation of the parameters, especially for the shape parameter which is highly influential in estimating the hazard levels and high return periods."

Fig 3 correct ":,"
Corrected

P7 l4 I would write: "The largest observed AFI..."
I have deleted this sentence since this is discussed later on.

Table1 caption. “Cell id”?
Corrected

P9 l1 Please, use “The probability density function (pdf) of X, ...”. Also later you talk about “densities”. Later, I suggest using pdf.
Corrected

P9 l6 “copula density” instead of “copula function”?
Corrected

P10 l10 “eq 2 and 10” should be eq 2 and 3.
Corrected

P10 l14. Is this only an intuition? Anyway, you might rephrase.
I changed this to “based on the premise”.

P10 l15 Please, define what a tree is, as it would help the reader. You might “use” the 4-dim example to explain what a tree and a first tree are. You might consider using the term “tree” or “level” only in the full text, as you refer to the same thing with these two different words, and this might confuse the non-expert reader (e.g., p10 l23-24).

I have added a figure 6 showing the tree for the 4-d case to make this more clear. I am also referring always to trees and not levels in the revised manuscript to reduce the confusion.

P11 l6 “largest contribution at the second level”. Add something like “after the independent copula”.
I have delete this sentence.

P17 l15 average AFI, please: add (mAFI)
Corrected

P17 l20 “However, the non-stationary fits were statistically similar to the stationary ones, with $\beta 1$ parameters not significantly different from zero.”
You might write: “Despite the significant anticorrelation found between the average AFI (mAFI) and the NAOI, the non-stationary fits were statistically similar to the stationary ones, with $\beta 1$ parameters not significantly different from zero.”
Then the next sentence (“This is probably related to the quite noisy character of the phenomenon and the relatively short historical record used in this study, which makes it difficult to discern the statistical differences in the extreme temperatures between positive and negative NAO winters”) could be rephrased, maybe explicitly referring to the noise as a function of the spatial scale (in fact, the noise is not visible when looking at the average AFI (mAFI), as the correlation between mAFI and NAOI is about -0.6).
I have included the NAOI in the new model – this has been possible after a bug fix, via the implementation of a P0 model, and also due to the longer Reanalysis data set.

P19 l10 (a) and (c) are pretty similar: you might unify them. Furthermore, as previously discussed, the the full multivariate pdf (marginals and copula) has uncertainties, and not only the copula (RVM) (as it looks from c).
Indeed these are now unified.
P20 l13
In these cases (fig8b), is the RVM structure always the same as the RVM structure used in the full study so far? Are there independent copulas in the RVMs used for the sensitivity study? Please, very briefly specify these details.

The sensitivity tests had different RVM structure but included the independent copulas. However, I have deleted this section from the revised manuscript mainly due to computational reasons but also I don't believe they were adding much into the article (i.e. the results were following the theoretical tail dependences).

Here I paste a comment I gave in the previous revision. This might be useful, given the comment I have written in this review.
"The 10,000 years time series should be long enough to neglect uncertainties associated with the Monte Carlo simulations (which is the method used for extracting the return period associated with the fitted parametric pdf) (Serinaldi et al. (2015) and Bevacqua et al. (2017)). [One should ensure if the sample is "long enough" via repeating the (10,000 years) simulations several times and checking if the there are differences in the estimated return period (if there are no differences, the 10,000 years sample is long enough)]. Performing a long enough simulations allows one to get a convergence to the true return period that one would get analytically from the fitted pdf (given the complexity of the problem it is impracticable to get an analytical derivation of the RP). Performing a long simulation does not solve the issue about the model uncertainties (uncertainties existing about the pdf), which is there because the pdf is calibrated on a finite - very short - sample. I suggest to discuss this in a way to make difference between these different type of uncertainties. "
Best regards.

A hazard model of subfreezing temperatures in the United Kingdom using vine copulas

Symeon Koumoutsaris

Guy Carpenter, Tower Place, London, EC3R 5BU, UK

Correspondence to: Symeon Koumoutsaris (symeon.koumoutsaris@guycarp.com)

Abstract. Extreme cold weather events, such as the winters of 1962/63, the third coldest winter ever recorded to the Central England Temperature record, or more recently the winter of 2010/11, have significant consequences for the society and economy. This paper assesses the probability of such extreme cold weather across the United Kingdom. For that, a statistical model is developed in order to model the extremes of the Air Freezing Index (AFI), which is a common measure of magnitude and duration of freezing temperatures. A novel approach in the modelling of the spatial dependence of the hazard has been followed which takes advantage of the vine copula methodology. The method allows to model complex dependencies especially between the tails of the AFI distributions which is important to assess ~~reliably~~ the extreme behaviour of such events. The influence of North Atlantic Oscillation (NAO) and of anthropogenic climate change on the frequency of UK cold winters has also been taken into account. The model suggests that the ~~extreme winter 1962/63 has a return period of approximately once every 89 years, with 95% confidence intervals between 81 to 120 years.~~ occurrence of such extreme cold events have increased approximately two times during the course of the 20th century as a result of anthropogenic climate change. Furthermore, the model predicts that such an event will become quite uncommon, about 10 times less frequently, under a 2xCO_2 climate scenario. The frequency of extreme cold spells in UK has been found to be heavily modulated by NAO, as well. A cold event is estimated to occur ≈3-4 times more likely during its negative than its positive phase. However, the ~~relative~~ estimated uncertainty in these results is quite large and comes from the relatively short record length~~together with the unclear effects of anthropogenic forcing on the local climate~~. Moreover, possible spurious trends in the historical data add considerable uncertainty to ~~this estimate. This model is used as part of a probabilistic catastrophe model for insured losses caused by the bursting of pipes~~these estimates, as well.

1 Introduction

Extended periods of extreme cold weather can cause severe disruptions in human societies; on human health, by exacerbating previous medical conditions or due to reduction of food supply which can lead to famine and disease; agriculture, by devastating crops ~~particularily~~ particularly if the freeze occurs early or late in the growing season; on infrastructure, e.g. severe disruptions in the transport system, burst of residential or system water pipes (**?**). All these consequences lead to important economic losses.

Of particular interest for the insurance industry are the economical losses that originate as a result of bursting of pipes due to freeze events. Water pipes burst because the water inside them expands as it gets close to freezing which causes an increase in pressure inside the pipe. Whether a pipe will break or not, depends on the water temperature (and consequently on the air temperature), the freezing duration, the pipe diameter and composition, the wind chill effect (due to wind and air leakage on water pipes), and the ~~presense~~ presence of insulation (**??**).

Insurance losses from burst pipes have a significant impact on the UK insurance industry. They amount to more than £900 million in the last 10 years, representing around 10% of the total insured losses, mainly due to flood and windstorm, in the United Kingdom (UK) during the same period (**?**). Particular years can be very damaging, such as, for example, the winter of 2010/2011 where losses from burst pipes have exceeded £300 million in UK making it the peril with the largest losses that year (**?**). Moreover, much more extreme cold winters have actually occurred in the UK in the last 100 years, such as the winters of 1946/47 and 1962/63. It is crucial for the insurance business to be able to anticipate the likelihood of occurrence of similar and even more extreme events so that they can adequately prepare for their financial impact (**?**). In fact, the capital requirements in (re)insurance is estimated in a 1 in 200 year return period (RP) loss basis, which is usually much larger than the available historical records.

Probabilistic catastrophe modelling is generally agreed to be the most appropriate method to analyze such problems. The main goal of catastrophe models is to estimate the full spectrum of probability of loss for a specific insurance portfolio (i.e. comprised by several residential, auto, commercial or industrial risks). This requires the ability to extrapolate the possible losses at each risk to high return periods (RP) which is usually achieved by simulating synthetic events that are likely to happen in the near future (typically a year). More importantly, it requires to consider also how all risks relate to each other and their potential synergy to create catastrophic losses. Such spatial dependence between risks can result from various sources, for example due to the spatial structure of the hazard (e.g. the footprint in a windstorm or the catchment area in a flood event) or due to similar building vulnerabilities between risks in the same geographical area (e.g. due to common building practices) (**?**).

Modelling the spatial dependence of the hazard is usually achieved by taking advantage of certain characteristic properties of the hazard footprint, like for example the track path and the radius of maximum wind for ~~and~~ windstorms or the elevation in the case of floods. In the case of temperature, however, such a property cannot be easily defined; an alternative solution is to use multivariate copula models. Based on Sklar's theorem (**?**), the joint distribution of all risk sources can be fully specified by the separate marginal distributions of the variables and by their copula, which defines the dependence structure between the variables.

However, one important difficulty is the limited choice of adequate copulas for more than two dimensions. For example, standard multivariate copula models such as the elliptical and Archimedean copulas do not allow for different dependency models between pairs of variables. Vine copulas provide a flexible solution to this problem based on a pairwise decomposition of a multivariate model into bivariate copulas. This approach is very flexible, as the bivariate copulas can be selected independently for each pair, from a wide range of parametric families, which enables modelling of a wide range of complex dependencies (**??**).

In this paper, the vine copula methodology is used in a novel application to develop a catastrophe model on insurance losses due to pipe bursts resulting from freeze events in the United Kingdom. The focus here is on the hazard component (Sect. 2) which is modeled using the Air Freezing Index (AFI), an index which takes account both the magnitude and duration of air temperature below freezing, calculated from ~~temperature~~ reanalysis data from the last ~~51~~ 110 years. The ~~methods used~~ statistical models utilized to extrapolate to longer return periods are described in Sect. 3. ~~Extreme value analysis is performed on the historical AFI values in order to extrapolate to longer return periods (Sect. 3.2).~~ The model also accounts for two major drivers of climate variability in UK that are incorporated as predictors:

- the North Atlantic Oscillation (NAO), a leading pattern of weather and climate variability over the entire Northern Hemisphere, which accounts for more than half of the year-to-year variability in winter surface temperature over UK.
- Anthropogenic climate change and its direct effects in the temperature profile in the UK.

Stochastic winter-seasons are simulated taking into account the correlation of the hazard between all pair-cells with the help of regular vine copulas (Sect. 3.3). The resulting return periods of extreme cold winters in UK, including the underlying uncertainties, are discussed in Sect. 4. Concluding remarks are found in Sect. 5.

2 ~~Temperature data~~Data

2.1 Temperature data sets

The hazard component of the catastrophe model is based on the ~~gridded dataset of observed daily average temperature developed from the UK Met Office (?). The dataset covers the entire UK for the period from 1960 to 2011 at 5km x 5km resolution and georeferenced in the British National Grid projection. It is based on temperature data retreived from 540 stations accross UK with an average station density of 21 x 21 km^2 (??). The data are rigorously quality-checked and interpolated to a regular grid using inverse-distance weighting, as described in ?. The dependencies across cells, may, thus, be partially due to the interpolation itself~~European Centre for Medium-Range Weather Forecasts (ECMWF) twentieth century reanalysis (ERA-20C) covering the entire twentieth century from 1900 to 2010 (?). Reanalyses are data-assimilating weather models which are widely used as proxies for the true state of the atmosphere in the recent past. Even though centennial reanalyses, such as ERA-20C, represent the most convenient data sets for assessing the long-term historical climate, biases and uncertainties inherent in both raw observations and models mean that they should be used with caution.

For consistency throughout the period, the observational input in ERA-20C is limited to surface pressure and surface marine winds only, which may however lead to some reduction in accuracy (?). For example, important differences in the 2-meter temperature have been found between ERA-20C and other centennial reanalysis data sets, especially during the first half of the twentieth century as a result of the spare observational network in those early years (??). Furthermore, studies have suggested that long-term changes in the Arctic Oscillation, mean sea level pressure, and wintertime storminess seen in ERA-20C, may be spurious as a result of the assimilation of increasing numbers of observations (???).

~~For computational reasons, the data are regridded to a lower resolutionof 50 km x 50km, which leads~~ ERA-20C product provides daily 3-hour forecast (i.e. eight forecast steps starting at 06:00UTC each day) of minimum and maximum temperature at 2 meters. These are used to compute daily minimum and maximum values at every grid cell for the entire period. The daily average temperatures are then computed as 0.5(T_{max}-T_{min}) and the data re-gridded to a 1°x1°resolution, which corresponds to a total of ~~170~~ 67 cells over land. ~~The use of a coarser~~

The coarse horizontal resolution is expected to have relatively small influence in most cases given that winter climate anomalies are often coherent across large parts of the UK as they are primarily associated with large-scale atmospheric circulation patterns (**?**). Nevertheless, local temperature may be subtly different in certain micro-climates, such as upland and urban regions. In particular over urban regions, which are most important from an insurance perspective, lower resolution may lead to temperatures that are biased towards lower values, leading though to a conservative view on the severity of extreme freeze events. In upland regions, on the other hand, extreme cold temperatures are most probably underestimated, although it is reasonable to expect that their damaging effects are somewhat mitigated from increased protection levels. For example, water pipes in properties located in ~~mountaineous~~ mountainous regions are usually better protected against cold spells.

For comparison purposes, the observed daily average temperature gridded data set developed from the UK Met Office is also used (**?**). This data set is based on temperature data retrieved from 540 stations across UK with an average station density of 21 x 21 km^2 (**??**). It covers the entire UK, but for a much shorter period of 51 years (1960-2011). The original 5km x 5km resolution is re-gridded using bi-linear interpolation to 1°x1°in order to match the ERA-20C grid.

2.2 North Atlantic Oscillation Index

The NAO refers to a redistribution of atmospheric mass between the Arctic and the subtropical Atlantic, and swings from one phase to another producing large changes in weather, and in particular in surface air temperature, over the Atlantic and the adjacent continents (**?**). It is described by the NAO index (NAOI), a measure of the mean atmospheric pressure gradient between the Azores High and the Iceland Low. A positive NAOI is associated with depression systems taking a more northerly route across the Atlantic, which causes UK weather to be milder, while a negative NAOI is associated with depression systems taking a more southerly route, as a result of which UK weather tends to be colder and drier (**?**). In this study, the winter (December thru March) station-based index of the NAO from **?** is used, which is based on the difference of normalized sea level pressure between Lisbon, Portugal and Stykkisholmur/Reykjavik, Iceland (Figure 1b).

2.3 Anthropogenic forcing

Increases in concentration of greenhouse gases, such as carbon dioxide (CO_2), are accompanied by increased radiative forcing, i.e. the difference between the incoming radiation from the sun and the outgoing radiation emitted from the Earth. This forcing arises from the ability of the gases to absorb long wave radiation, thus reducing the amount of heat energy being lost to space, and increasing the warming of the earth's surface. Here we use the change in radiative forcing from CO_2 as a predictor for climate change. It is calculated using the simplified expression (**?**):

$$\Delta F_{CO_2} = 5.35 ln\left(\frac{C_i}{C_{1990}}\right) \tag{1}$$

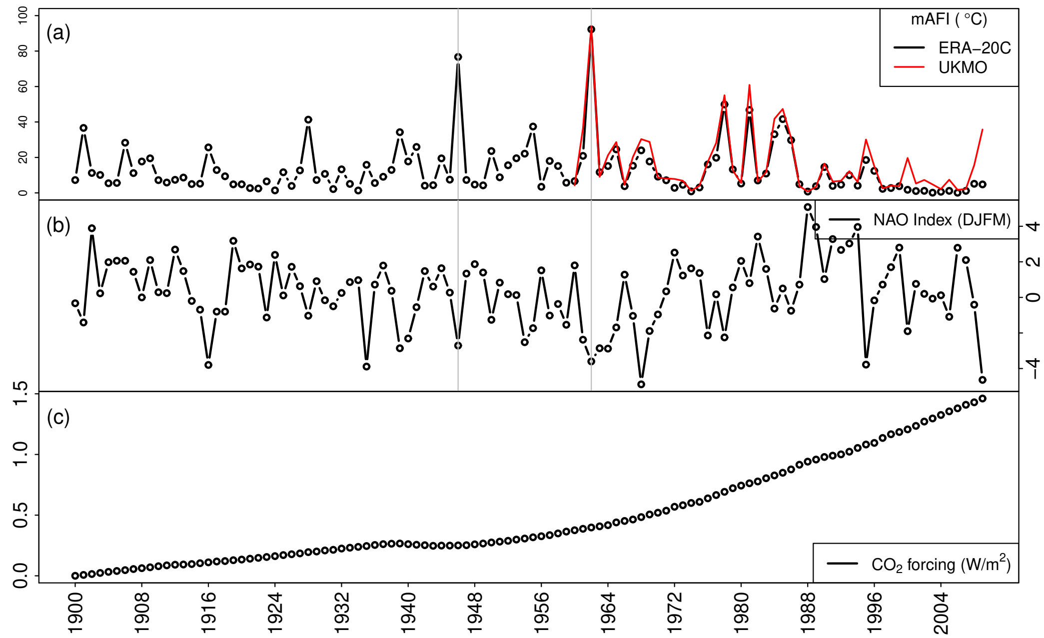

Figure 1. Interannual variation of (a) average AFI over UK (mAFI), (b) the North Atlantic Oscillation Index (NAOI), and (c) CO_2 forcing during the study period.

where ΔF_{CO_2} is the radiative forcing change (in W m^{-2}), C_i is the concentration of atmospheric CO_2 at year i, and C_{1900} is the reference 'pre-industrial' CO_2 concentration at year 1900. Consequently, a doubling of CO_2 corresponds to a change in the radiative forcing of 3.7 W m^{-2}. Historical observations of global mean CO_2 concentrations (in parts per million or ppm) are based on **?**. The temporal increase in the CO_2 radiative forcing during the 20th century is shown in Figure 1c.

3 Methods

3.1 Air-Freezing Index and historical events

The daily temperature ~~gridded~~ data are used to compute the AFI at each grid cell, as the sum of the absolute average daily temperatures of all days with below 0°C temperatures during the freezing period (~~1)~~Eq. (3)). The freezing period in this study is defined from first of June of year y to end of May of the following year $y+1$, in order to include the entire winter season. Because AFI accounts both for the magnitude and duration of the freezing period, it is commonly used for determining the freezing severity of the winter season (**??**).

$$AFI_i = \begin{cases} \sum_{day=1/6/(y)}^{31/5/(y+1)} |T_{day}|, & \text{if } T_{day} < 0°\text{C} \\ 0, & \text{if } T_{day} \geq 0°\text{C for all days in year } y \end{cases} \quad (2)$$

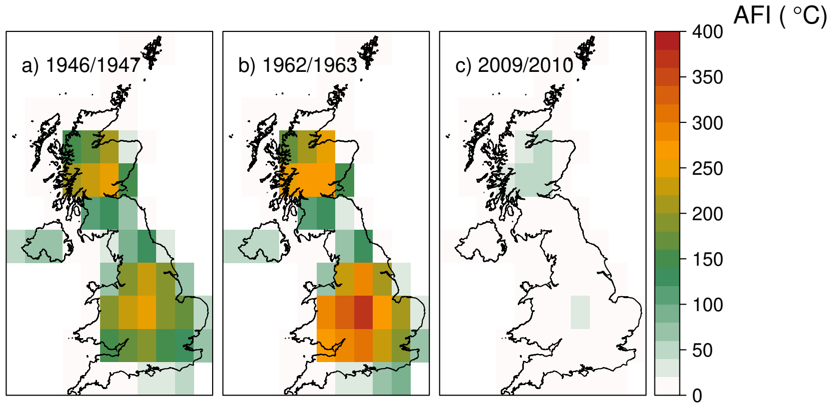

Figure 2. Map of AFI values (in °C) for the the winter-seasons of a) ~~1962~~1946/~~63~~47, b) ~~2009~~1962/~~10~~63, and c) ~~2010~~2009/~~11.~~10.

~~Figure 1a shows a map of the AFI values for the season~~ Maps of AFI values from ERA-20C for the severe winters of 1946/47, 1962/~~1963~~ 63, and 2009/10 are shown in Figure 2. The winter of 1946/47 (i.e. season starting from 1st June ~~1962~~ 1946 to 31st of May ~~1963) , which was~~ 1947) was a harsh European winter noted for its impact in the United Kingdom. It was notable for a succession of snowstorms from late January until mid-March, mainly associated with easterly airstreams (**?**). The mean AFI value (mAFI) in the entire UK (i.e. average of AFI values across all gridcells) mounted up to 75.6°C, the second largest value during the period.

The 1962/1963 winter season was the most severe winter in the 20th century and one of the coldest on the record in the United Kingdom (**?**). The "Big Freeze of 1962/63", as it is also known, began on the 26 of December 1962 with heavy snowfall and went on for nearly three months until March 1963. The cause of the cold conditions has been the development of a large "blocking" anticyclone over Scandinavia and north-western Russia. Easterly winds on the southern edge of this system transported cold continental air westwards, displacing the more usual mild westerly influence from the Atlantic Ocean on the British Isles. Over the Christmas period, the Scandinavian High collapsed, but a new one formed near Iceland, bringing Northerly winds. The ~~mean AFI value (mAFI)~~ mAFI in the entire UK (i.e. average of AFI values across all gridcells) mounted up to ~~98.3~~90.9°C, which represents ~~four~~ six standard deviations larger than the average of the entire ~~51-year period (19.6~~110-year period (14.0°C). The event affected ~~the entire country with peak AFI values exceeding 200C both in the South and in the North~~ more the Southern part of the country ~~(Fig. 1)~~as shown in Fig. 2.

After 1962/63, a long run of mild winters followed until late 1978 and early ~~1979 (Fig. 2).~~ 1979. However, temperatures in 1978/79 were not as low and the cold weather was interrupted frequently by brief periods of thaw (**?**). The mAFI value of winter 1978/79 reached ~~59.2~~49.2°C. The 1980s stands out as a decade with several cold spells in UK, with mAFI values above ~~40~~30°C for the winters 1981/82, 1984/85, and 1985/86 (~~64.8, 43.9, and 50.6~~ 46.1, 32.6, and 41.0 °C, respectively). ~~Finally, the winters~~

For the last 10 years of our study period (from 2000 to 2010), mAFI seem to be underestimated in the re-analysis data set (Fig. 1a). In particular, the winter of 2009/2010~~and 2010/2011~~ , which is well known to have brought frigid temperatures to ~~parts of Europe and the UK (???), with mAFI values across UK of 39.1 and 62.2~~the UK (????), has a mAFI value of only 4.7 °C (~~Fig. 1b and c)~~ Figure 2c) which is much lower than the long-term average (13 °C) and over ten times lower than mAFI value according to the UKMO dataset (59.1 °C). No clear reason is known for this bias, but it might be related to possible spurious long-term trends in the atmospheric circulation (?).

As shown in Figure 1a, the two most severe winters in the century (1946/47 and 1962/63) were associated with a negative NAO phase (??). As mentioned ~~previously, the latter one had a significant financial impact on the UK insurance industry. The relation between cold winter spells and the North Atlantic Oscillation (NAO), a large-scale mode of natural climate variability, is discussed in detail in Sect. 4.2.3.~~ earlier, the NAO has a profound effect on winter climate variability around the Atlantic basin, accounting more than half of the year-to-year variability in winter surface temperature over UK (??). Not surprising, the ERA-20C mAFI over the entire UK is found to be significantly anti-correlated (ρ = -0.49, pval=6.510^{-8}) with NAOI. A negative correlation is found between mAFI and ΔF_{CO_2} forcing, but it is much less significant (ρ = -0.17, pval= 0.08). Both NAO and climate change effects are included in the statistical model as predictors in order to account for their relation to cold winter spells in UK as discussed in the following section.

~~Interannual variation of UK average AFI over the study period. The North Atlantic Oscillation Index (NAOI) is also shown in dotted line.~~

3.2 Extreme value analysis

3.2.1 Stationary model

Since the historical data only extends for ~~51~~ 110 years and our interest lies in very rare events (such as 1 in 200 years), it is necessary to extrapolate by fitting an extreme value distribution. The Generalized Extreme Value (GEV) family of distributions has been chosen, which includes the Gumbel, the Fréchet, and Weibull distributions. An additional term was included, the probability of no hazard (P0), in order to account for the cells, mainly on the south England coast, that have years with no negative temperatures at all. The probability therefore that the AFI value (X) inside a cell j ~~will exceed~~ is lower or equal than a certain value (x) takes the form:

$$F(x) = P(X \leq x) = P0 + (1 - P0)exp\left\{ -\left(1 + \xi\frac{x - \mu}{\sigma}\right)^{-\frac{1}{\xi}}\right\} \quad (3)$$

where μ, σ, and ξ represent the location, scale, and shape parameters of the distribution, respectively. ~~$P0$ is computed as total number of years with no hazard/total number of years + 1.~~ $F(x)$ is defined when $1+\xi\frac{x-\mu}{\sigma} > 0$, $\mu \in \Re$, $\sigma > 0$, and $\xi \in \Re$. Its derivative, the GEV probability density function $f(x)$ is given by:

$$f(x) = f(x) = \begin{cases} P0, & \text{if } x = 0 \\ (1-P0)\frac{1}{\sigma}\left[1+\xi\left(\frac{x-\mu}{\sigma}\right)\right]^{-\frac{1}{\xi}-1} exp\left\{-\left[1+\xi\left(\frac{x-\mu}{\sigma}\right)\right]^{-\frac{1}{\xi}}\right\}, & \text{if } x > 0 \end{cases} \tag{4}$$

There are various methods of parameter estimation for fitting the GEV distribution, such as least squares estimation, maximum likelihood estimation (MLE), probability weighted moments, and others. Traditional parameter estimation techniques give equal weight to every observation in the ~~dataset~~data set. However, the focus in catastrophe modeling is mainly on the extreme outcomes and, thus, it is preferable to give more weight to the long return periods. ~~I therefore use the~~ The Tail-Weighted Maximum Likelihood Estimation (TWMLE) method developed by ~~(?)~~ **?** is employed here in order to estimate the GEV parameters~~which introduces ranking dependended~~. This method introduces ranking depended weights ($w_{(r)}$) in the maximum likelihood. The weights are defined for each cell based on the historical winter-season AFI values, i.e. the lowest historical AFI value in the cell (rank r=1 out of n observations) has the lowest weight, while the largest historical AFI value (rank r=n) has the largest weight, as follows:

$$w_{(r)} = AFI_{(r)} / \sum_{r=1}^{n} AFI_{(r)} \tag{5}$$

Along with the TWMLE method described above, a second modification has been implemented in order to geographically smooth the GEV parameters. The smoothing is incorporated into the fitting process by minimizing the local (ranked) log-likelihood. More precisely, the log-likelihood at each grid cell ~~i~~ i is calculated using all grid points but weighted by their distance~~d_{ij}~~:

$$LogL_i = \sum_{j=1}^{170} (k_{ij} * LogL_j) \tag{6}$$

where $k_{ij} = \frac{1}{\sqrt{2\pi}} e^{-\frac{d_{ij}^2}{2L^2}}$, d_{ij} is the distance between cell i and j, L is the smoothing parameter, ~~and~~ $LogL_j$ is the ranked log-likelihood for cell ~~j~~j.

~~Because the historical gridded data are already geographically smoothed~~The smoothing increases the sample size at each grid point, which thus leads to a more precise estimation of the parameters, especially for the shape parameter which is highly influential in estimating the hazard levels and high return periods. Because the data grid resolution is already coarse, a small length scale parameter L of ~~15~~ 20 km has been used (in comparison to the ~~50km~~ grid size). ~~In general, the increase of the sample size at each grid point allows for a more precise estimation of the parameters, especially for the shape parameter which is highly influential in estimating the hazard levels and high return periods.~~

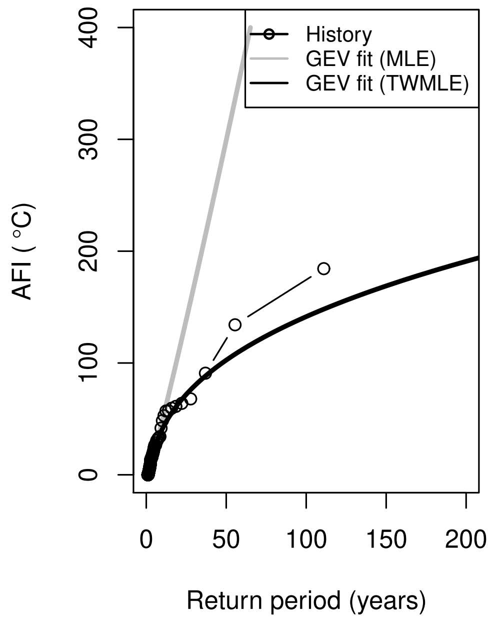

Figure 3. AFI return period curves for a single cell over London: ~~,~~ empirical fit (black circles)~~empirical fit~~, ~~(grey line)~~ GEV fitted with MLE ~~, and~~ (~~black~~ grey line), and GEV fitted with TWMLE and geographical smoothing (black line).

Finally, in order to avoid an over-estimate of the positive value of the shape parameter due to the small sample size (**?**), a modification of the maximum likelihood estimator using a penalty function is also applied for fitting the GEV. The penalty function penalizes estimates of ξ that are close to, or greater than 1, following **?**.

Estimates of P0 for each grid cell are obtained by fitting a logistic regression model with intercept only (Eq. (7)). As before, the fitting is performed against all grid cells, weighted by their distance d_{ij}, and a length scale of 20 Km has been used. The model is extended in the non-stationary model to include covariates as described in Sect. 3.2.2.

$$ln\left(\frac{P0}{1-P0}\right) = b_0 \qquad (7)$$

As an example, the GEV fit for a single cell over London is shown in Fig. 3. The curve fitted as described above (black line) is closer to the empirical estimates (black circles, computed as described in Sect. 4.1) in comparison with the GEV fit with no weighting applied (grey line). As shown in table 1, for both fits the shape parameter is positive (i.e. both fits correspond to the Fréchet distribution), but for the approach followed here (TWMLE + geographical smoothing), the shape parameter is smaller leading to a shorter tail and a curve that is nearer to the empirical estimate. ~~The largest AFI empirical point in this figure~~

Table 1. ~~GEV~~ Model parameters for a single cell over London~~(cellid = 32)~~.

method	~~location~~ b_0	~~scale~~ b_1	~~shape~~ b_2	~~P0~~ μ	μ_0	μ_1	σ	ξ
MLE (no predictors)	~~3.53~~ -1.77	~~5.12~~ 0	~~1.14~~ 0	~~0.12~~ 4.05	0	0	5.61	1.08
TWMLE + geographical smoothing (no predictors)	~~5.33~~ -1.77	~~12.05~~ 0	~~0.28~~ 0	~~0.12~~ 4.87	0	0	12.67	0.35
TWMLE + geographical smoothing (with predictors)	-3.74	0.36	2.62	-2.27	-5.87	3.07	15.32	0.25

~~represents the 1962/63 exceptional winter which is estimated to be a more rare event than what the historical data suggests (i.e. larger than 1 in 52 years), as further discussed in the following sections.~~

Maps of the fitted parameters are shown in Fig. 4. The probability of non-negative temperatures during a season (P0) is, as expected, larger around the coast which has milder and less variable climate due to the water influence. This also explains the lower mean (location parameter) and larger spread (scale parameter) in the AFI distributions around the coast in comparison to inland. The shape parameter, which affects the skew of the distribution, shows larger values in the southern part of the UK in comparison to the north, suggesting a less rapid increase in the maximum AFI estimates.

3.2.2 Non Stationary model

In stationary models, the distribution parameter space is assumed to be constant for the period under consideration. However, such assumption is not valid in the presence of atmospheric circulation patterns or anthropogenic changes. In this study, a generalized linear model (GLM) is introduced into the statistical distribution parameter estimates in order to improve the non-stationarity representation of the model. The influence of NAO and of global warming is examined by exploring improvements to the distribution fits, after incorporating linear covariates on the distribution parameters.

- $ln\left(\frac{P0}{1-P0}\right) = b_0 + b_1 NAOI + b_2 \Delta F_{CO_2}$
- $\mu = \mu_0 + \mu_1 NAOI + \mu_2 \Delta F_{CO_2}$

where (b_0, μ_0) are the stationary model parameter estimates and (b_1, μ_1), (b_2, μ_2) are linear transformations of the covariates NAOI and ΔF_{CO_2} with respect to time, respectively.

In this study, only non-stationarity with respect to P0 and the location parameter, μ, is discussed, since modeling temporal changes in σ and ξ reliably requires long-term observations in order to be estimated accurately (**??**). A simple linear model is selected as this is usually preferred when searching for trends in the occurrence of extreme events (**?**). Finally, even though some climate modeling studies predict changes in the nature of NAO variability in an increasing CO_2 climate (**??**), the model does not include any interaction-terms, as they have been found to be non-significant.

As before, the parameters of each cell are estimated taking also into account its neighboring cells weighted by their distance. The most pertinent model is selected, for each cell, using the χ^2 test, based on the change in deviance, between the null, one or two predictor model. If the significance value is less than 0.01, the model is estimated to have a significant improvement over

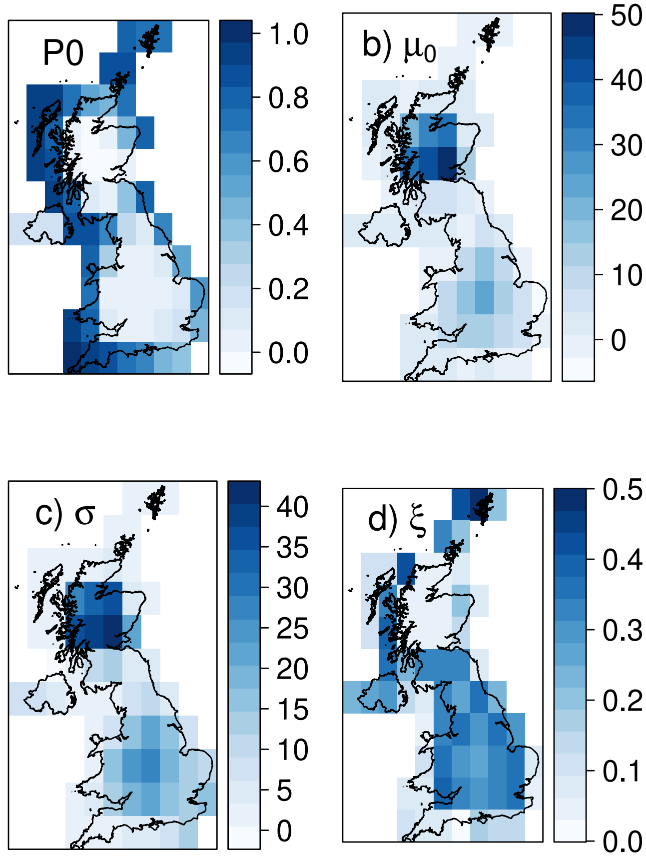

Figure 4. Maps showing the spatial distribution of the model fitted parameters: a) P0 calculated as $e^{b_0}/(e^{b_0}+1)$, b) location μ, c) scale σ, and d) shape ξ.

the reduced model. A separate test is performed for the P0 and the GEV model. As an example, in the case of the London cell, the model with two predictors for both P0 and the location parameter has been chosen (table 1).

The spatial distribution of the parameters of the final model is shown in Fig. 5. Increasing NAOI or ΔF_{CO_2} are consistent with a warming trend, leading to positive values of the P0 parameters (indicating increases in the number of years with no negative temperatures) and to negative values in the location parameters (indicating lower means in the AFI distributions). The NAO is found to affect more cells in total (90%) in comparison to anthropogenic climate change (51%). Notice however that due to the internal variability of the NAO, any signal from a climate change trend can be hidden in the limited observational period.

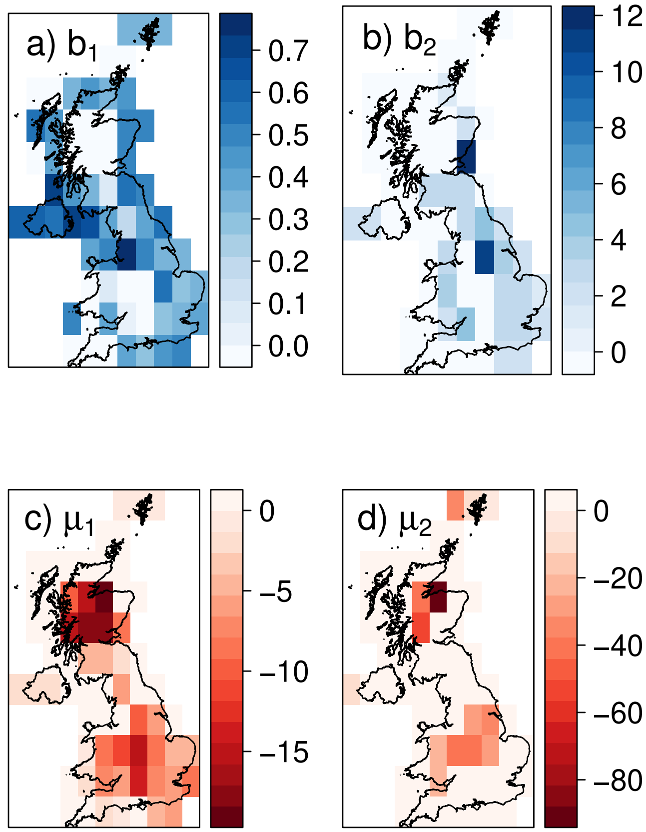

Figure 5. Maps showing the spatial distribution of the non-stationary model parameters: a) b_1, b) b_2, c) μ_1, and d) μ_2. Zero values indicate linear trends not significant at the 0.01 level.

3.3 Copulas and vine copulas

The stochastic behaviour of the hazard (i.e. AFI) at each cell is fully described by its corresponding GEV probability distribution, as described in Sect. 3.2. However, insurance portfolio loss analysis requires the calculation of the combined stochastic behaviour of the hazard across all the model domain (i.e. all cells). This is described by the joint distribution of the hazard which, according to Sklar's theorem, can be fully specified by the separate marginal GEV distributions and by their (d-dimensional) copula, which models the hazard dependence between the cells.

More precisely, consider a vector of $X = (X_1,...,X_d)$ of random variables with a joint probability density function (pdf), $f(x_1,...,x_d)$. Sklar's theorem (**?**) states that any multivariate continuous distribution function $F(x_1,...,x_d)$ with marginals $F_1(x_1),...,F_d(x_d)$ can be written as:

$$F(x_1,...,x_d) = C(F_1(x_1),...,F_d(x_d)) \tag{8}$$

for some appropriate d-dimensional copula C, which is uniquely determined on $[0,1]^d$.

The ~~density~~ probability density function (pdf) of X, $f(x_1,...,x_d)$, can be found by taking the partial derivatives with respect to X:

$$f(x_1,...,x_d) = c(u_1,...,u_d)\prod_{i=1}^{d} f_i(x_i) \tag{9}$$

where $c(u_1,...,u_d)$ is the copula density, given by

$$c(u_1,...,u_d) = \frac{\vartheta^d C(u_1,...,u_d)}{\vartheta u_1 ... u_d} \tag{10}$$

Expression ~~6~~ 9 is important in terms of modelling because it permits to define a multivariate density as the product of marginal ~~densities~~ pdfs and a copula density function that captures the dependence between the random variables (**?**). For a theoretical introduction to copulas, see **????**; for a practical/engineering approach and guidelines, see **????**

To quantify the dependence between variables, different measures have been defined, addressing different aspects of dependence. A common measure of overall dependence is the Kendall rank correlation coefficient, commonly referred to as Kendall's τ coefficient (**?**). However, dependence of rare events cannot be measured by overall correlations: even if two variables are completely uncorrelated, there can be a significant probability of a concurrent extreme event in the two, i.e., they can still be tail dependent. Tail dependence describes the amount of dependence in the lower tail or upper tail of a bivariate distribution. For its mathematical definition see **?**.

One important complication is that identifying the appropriate d-dimensional copula is not an easy task. In high dimensions, the choice of adequate families is rather limited (**?**). Standard multivariate copulas, either do not allow for tail dependence (i.e. multivariate Gaussian) or have only a single parameter to control tail dependence of all pairs of variables (Student-t and ~~archimedean~~ Archimedean multivariate copulas). This is ~~particularily~~ particularly problematic for catastrophe modeling applications, where a flexible modeling of tails is vital to assess reliably the extreme behaviour of natural events.

Vine copulas provide a flexible solution to this problem based on a pairwise decomposition of a multivariate model into bivariate (conditional and unconditional) copulas, where each pair-copula can be ~~choosen~~ chosen independently from the others. In particular, asymmetries and tail dependence can be taken into account as well as (conditional) independence to build more parsimonious models. Vines thus combine the advantages of multivariate copula modeling, that is separation of marginal and dependence modeling, and the flexibility of bivariate copulas (**?**).

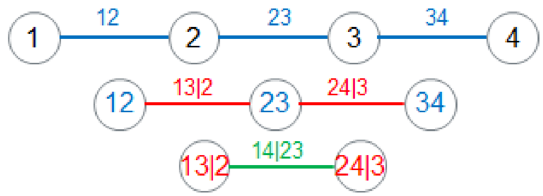

Figure 6. Example of 4-dimensional R-Vine trees corresponding to the decomposition shown in Eq. (11).

As an example, in a 4-dimensional case, the joint pdf can be decomposed as a product of 6 pair-copulas (3 uncoditional and 3 conditional) and 4 marginal ~~densities~~ pdfs as shown in Eq. ~~??~~(11):

$$
\begin{aligned}
f(x_1,x_2,x_3,x_4) = f(x_1)f(x_2)f(x_3)f(x_4) \\
\times c_{12}(F_1(x_1),F_2(x_2)) \\
\times c_{23}(F_2(x_2),F_3(x_3)) \\
\times c_{34}(F_3(x_3),F_4(x_4)) \\
\times c_{13|2}(F_{1|2}(x_1 \mid x_2)),F_{3|2}(x_3 \mid x_2))) \\
\times c_{24|3}(F_{2|3}(x_2 \mid x_3)),F_{4|3}(x_4 \mid x_3))) \\
\times c_{14|23}(F_{1|23}(x_1 \mid x_2,x_3)),F_{4|23}(x_4 \mid x_2,x_3)))
\end{aligned}
\tag{11}
$$

The above decomposition is not unique and **?** introduced a graphical structure called regular vine (R-Vine) structure to represent this decomposition with a set of nested trees. The dependence structure with three trees for the 4-dimensional example above is shown in Figure 6. More details on vine copulas can be found in **????**.

3.3.1 Selection of the Regular Vine Model (RVM)

In this study, the joint multivariate hazard distribution of AFI across all the model domain (~~170~~ 67 cells) is decomposed as a product of marginal and pair-copula ~~densities~~ pdfs (in a similar way as shown for the 4-d case above). F(x) and f(x) represent the ~~margnial~~ marginal GEV distributions here as defined by Eq. ~~3 and 4~~(3) and (4). The pair-copulas are fitted using the R (https://www.r-project.org/) package VineCopula (**??**). The method follows an automatic strategy of jointly searching for an appropriate R-Vine tree structure, its pair-copula families, and estimating their parameters developed by **?**. This algorithm selects the tree structure by maximizing the empirical Kendall's τ values, based on the ~~intuition~~ premise that variable pairs with high dependence should contribute significantly to the model fit and should be included in the first trees.

The copula family types for each selected pair in the first tree are determined by using the Akaike information criterion ~~(see (?))~~(**?**). For computational reasons, the two-parameter Archimedean copulas are excluded from this analysis, which however has only a negligible impact in the results ~~as discussed in Sect. ??.~~ (not shown). The copula parameters are estimated sequen-

Table 2. Percentage of family types used for the first five ~~levels~~ trees of the R-Vine Model.~~Results for all levels can be found in the supplementary material.~~

Tree	Indep	Gaussian	Student t	Clayton	Gumbel	Frank	Joe	180°Clayton	180°Gumbel	180°Joe	90°Clayton	90°Gumbel	90°Joe	270°Clayton	270°Gumbel	270°Joe
1	0	3.0	51.5	0	34.8	1.5	1.5	1.5	0	6.1	0	0	0	0	0	0
2	9.2	4.6	36.9	3.1	6.2	16.9	1.5	3.1	1.5	0	1.5	4.6	7.7	0	0	3.1
3	25	1.6	31.2	4.7	1.6	7.8	1.6	0	1.6	9.4	6.2	3.1	1.6	1.6	0	3.1
4	27	6.3	28.6	4.8	1.6	9.5	4.8	3.2	1.6	4.8	1.6	1.6	1.6	0	1.6	1.6
5	27.4	8.1	24.2	4.8	1.6	9.7	1.6	6.5	6.5	1.6	0	1.6	1.6	1.6	0	3.2
All	59.2	3.9	9.4	2.5	2.1	8.9	1.4	2.5	1.0	1.4	1.6	0.6	1.3	1.8	0.8	1.4

tially (using maximum likelihood estimation) starting from the top tree until the last tree, as described in **?**. This approach only involves estimation of bivariate copulas and has been chosen since it is computationally much less demanding than joint maximum likelihood estimation of all parameters at once.

The percentage of family types used for the first few trees of the selected RVM is shown in Table 2. The large majority of the pairs in all ~~levels~~ trees are estimated to be independent (~~64~~59%), but these pairs occur mainly at the higher ~~levels~~trees, since the most important dependencies are captured in the first trees (**??**). Large dependencies, with Kendall's tau coefficients greater than 0.90, are found as expected between ~~neighbouring~~ neighboring cells, but remain important across the whole model domain due to the nature of the hazard: AFI assess the freezing temperatures during the entire winter and, thus, is less associated with small scale local phenomena that can cause important spatial variation.

At the first tree, ~~48.5~~52% of the selected bivariate copulas are found to belong to the t-Student Copula and 35% to the Gumbel family, which exhibit positive dependence in the tails. Gumbel in particular has a greater dependence in the positive tail than in the negative and thus implies greater dependence at larger AFI values than at lower ones. ~~This is also the case for the 180° Clayton copula which has the largest contribution at the second level (9.5%), but with a much more uniform split between families. A sensitivity analysis on the influence of the selected copula families in the resulting return periods is presented in Sect. ??.~~ From the third tree and onwards, the percentage of independent families is always larger than 40%.

The small sample size used (~~51~~ 110 years of data) in conjunction with the high dimensions of the modelled pdf (~~170~~67) is of concern in this study since this can lead to large uncertainties in the resulting pdf, which can also propagate in the estimated return periods. ~~However, as discussed previously, the large majority of the pairs are estimated to be independent and the most important dependencies are captured at the first levels. Both together result in a virtual reduction in the dimensions of the pdf. Sensitivity analysis indicates that the first few trees of the RVM drive the majority of the dependencies, as further discussed in Sect. ??. Moreover, the~~ The impact of the short sample size on the uncertainties in the results is quantified using a bootstrap technique, as described in ~~the following section.~~ Sect. 3.3.2.

Goodness-of-fit (GOF) is calculated using the Cramer von Mises test, which compares the final selected RVM with the empirical copula. The RVineGofTest algorithm of the same R package implements different methods to compute the test, which however perform usually poorly in cases of small sample sizes and at higher dimensions as is the case for this work

Table 3. Goodness-of-fit values for the Cramer von Mises statistic based on ~~different methods~~ the empirical copula process (ECP) and based on the combination of probability integral transform and empirical copula process (ECP2) as implemented in the VineCopula R package.

Method	CvM	p.val

(**?**). Nevertheless, table 3 shows the GOF results for ~~each~~ two of these methods. ~~In all cases, the~~ The p.value is found to be larger than 0.05, which is an indication that the fitted RVM cannot be rejected at a 5% significance level. However, given also the quite large p.values, a Type II error cannot be excluded. Nevertheless, the suitability of the model, in comparison to the empirical data, is further discussed in the the results section as well.

3.3.2 Stochastic simulation and uncertainty estimation via parametric bootstrap

The RVM is used to simulate ~~10K~~ 100K years of winter-seasons in the UK. For each year, the simulated AFI values at each grid cell depend on the other cells based on the fitted RVM. ~~As an example, the AFI maps for the first six simulated winter-seasons are shown in Fig. 8.~~ Performing long enough simulations is necessary in order to obtain converged numerically results, i.e. to convergence to the "true" return period. Our focus here is the 200 year RP, which is commonly associated with capital and regulatory requirements. By repeating the simulation several times, it has been assessed that 100K years of winter seasons is long enough and the Monte Carlo simulation error is negligible.

The stationary model is used to generate a stochastic set which corresponds to the current hazard experience. The non-stationary model permits us to create additional stochastic sets that represent different climate conditions. In the case of NAO and following the Shapiro–Wilk test for normality, a 100-year long NAOI has been simulated assuming a Gaussian distribution (see Figure 7). In order to assess the influence of climate change in UK cold spells, three separate stochastic sets, of 100K years each, have been created as follows:

- Pre-industrial climate (ΔF_{CO_2}=0 Wm^{-2}), corresponding to pre-industrial (1900) concentration of CO_2 (296 ppm).
- Current climate (ΔF_{CO_2}=1.6 Wm^{-2}), corresponding to a present day (2018) concentration of CO_2 (400 ppm).
- Future double-CO_2 climate (ΔF_{CO_2} = 3.7 Wm^{-2}), corresponding to 2 x CO_2 concentration since pre-industrial times (592 ppm).

The small sample size used in this study (110 years of data) together with the high dimensions of the modelled pdf (67) can lead to large uncertainties in the estimated return periods. Following **?**, the model uncertainty is assessed using a parametric bootstrap approach, where a large number of models are created using as basis, instead of observations, randomly simulated data from the selected RVM. ~~The resulting uncertainty accounts for both the uncertainty in the selected RVM and the uncertainty associated with the 10K years of the Monte Carlo simulation.~~ In particular, confidence intervals are constructed as follows:

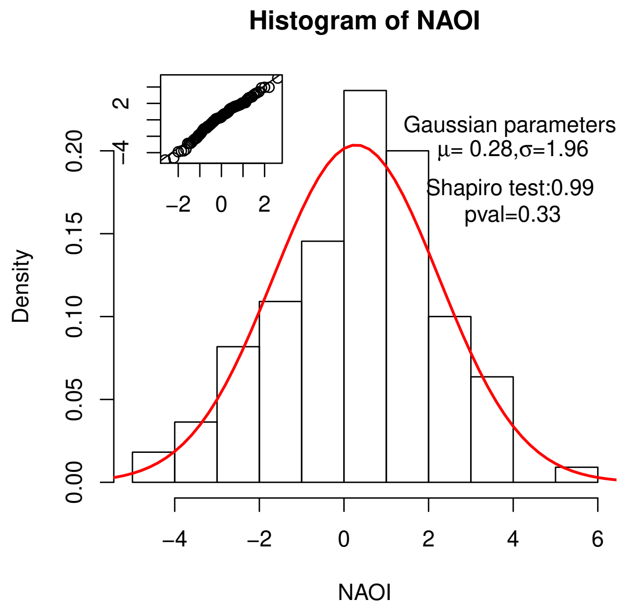

Figure 7. ~~AFI maps (in C) for~~ Histogram of the ~~first six (out~~ NAOI and the pdf of ~~10K) years of~~ the ~~stochastic set~~fitted Gaussian distribution (red line).

- A simulation with the same length as the observed data (i.e. ~~51~~ 110 years) is repeated for ~~1,000~~ B = 500 times.
- For each of these ~~1, 000 simulations, a new RVM is fitted , whose structure is the same as the selected RVM (i.e. the one fitted with the observed data), while the~~ B = 500 samples, a new full model is fitted (including new GEV and logistic regression model parameters at each cell and new RVM structure, pair-copula families and parameters~~are re-selected.~~) following the methodology described in Sect. 3.2.1 and 3.3.1.
- For each of the resulting ~~1,000~~ B = 500 RVMs, a simulation of 10K years of winter-seasons is performed. The uniform variables are then transformed using the (new) inverse marginal pdfs and the corresponding return period levels are estimated.
- The uncertainty in the return levels is estimated by identifying the 95% confidence interval (i.e. the range 2.5–97.5 %) from these ~~1,000~~ 500 return level curves.

~~The uncertainty associated solely due to the Monte Carlo sampling, is calculated as follows: Using the selected RVM, the simulation of~~ Due to computational constraints, confidence intervals are computed only for the stationary model and the simulation length has been reduced to 10K years ~~of winter seasons is repeated for 1,000 times. For each of these 1,000 simulations, the corresponding return period levels are calculated. The uncertainty in the return periods is estimated by~~

~~identifying the 95% confidence interval (~~(instead of 100K). In order to separate the uncertainty associated with the RVM only from the uncertainty of the full model, i.e. ~~the range 2.5–97.5 %) from these 1, 000 return level curves.~~ of the joint pdf, confidence intervals have been also calculated with the same approach as described above, but using the same marginal pdfs in each bootstrap repetition.

4 Results and discussion

4.1 Return period maps

~~The obtained GEV fits for each cell~~

The obtained stochastic sets (see Sect. 3.2) are used to create return period maps ~~, as shown in Fig. 4.~~ for the different climatic conditions. The top panels of Fig. 8 represent the AFI values that occur once every 10, 25, and 50 years ~~. The largest AFI values follow, as expected, the orography of UK peaking in the northern region of the highlands where the elevation reaches 1000 meters. In this region, values of AFI greater than 200C are reached often, approximately once every 5 years. The southern part of UK shows much lower values, not exceeding 200C even at the 50 year RP. Slightly milder temperatures are also evident around the London area denoting the urban micro-climate effect. Other urban regions (e.g. Manchester or Midlands area) do not stand out as much as a result of the low grid resolution.~~

~~(Top panels) Maps of AFI values (in C) for return periods of a) 1 in 10, b) 1 in 25, and c) 1 in 50 years calculated assuming a GEV distribution. (Bottom panels) Maps of the corrsponding empirical AFI values.~~

~~(Top panels) Maps of AFI values (in C) for return periods of a) 1 in 100, b) 1 in 200, and c) 1 in 500 years. (Bottom panels) Same as top panels but without taking into account the extreme winter of 1962/63.~~

based on the stationary model. The empirical return periods are also plotted for comparison (bottom panels~~, Fig. 4~~). These are calculated for each cell as 1/(1-P), where P represents the cumulative probabilities of the ranked values and is calculated based on the Weibull formula P=i/(n+1) (**?**). The ~~AFI values from the GEV fits correspond well with the empirical estimates, apart from the southern part of UK where the~~ spatial pattern is consistent between the empirical and stochastic sets, showing largest AFI values in high elevation areas, as expected. However, the empirical values are ~~approximately 20-30% larger at 50 years RP~~in general somewhat larger than the stochastic set. This difference is driven by the exceptional 1962/63 event which ~~empirically is estimated~~ is estimated empirically at 1 in ~~52 years while it is estimated~~ 110 years but is predicted to be less frequent according to the GEV fits. The probability of such an event happening today ~~and its influence in the inhabited areas~~ is discussed in detail in Sect. ~~4.2~~4.2.3.

~~At~~

Return period maps at higher return periods (100, 200, and 500 years~~, top panels of~~) for the pre-industrial, current, and $2xCO_2$ climate stochastic sets are shown in Fig. 5~~), AFI values exceeding 300C are predicted to be able to occur not only in the north but in the~~. UK in the beginning of the 20th century has been experiencing much colder winters than today. In a $2xCO_2$ climate change scenario, negative temperatures become very rare (larger than 1 in 500 years) in large part of the UK except at mountainous regions. It is also interesting to note that at high return periods and across all scenarios, larger AFI values are

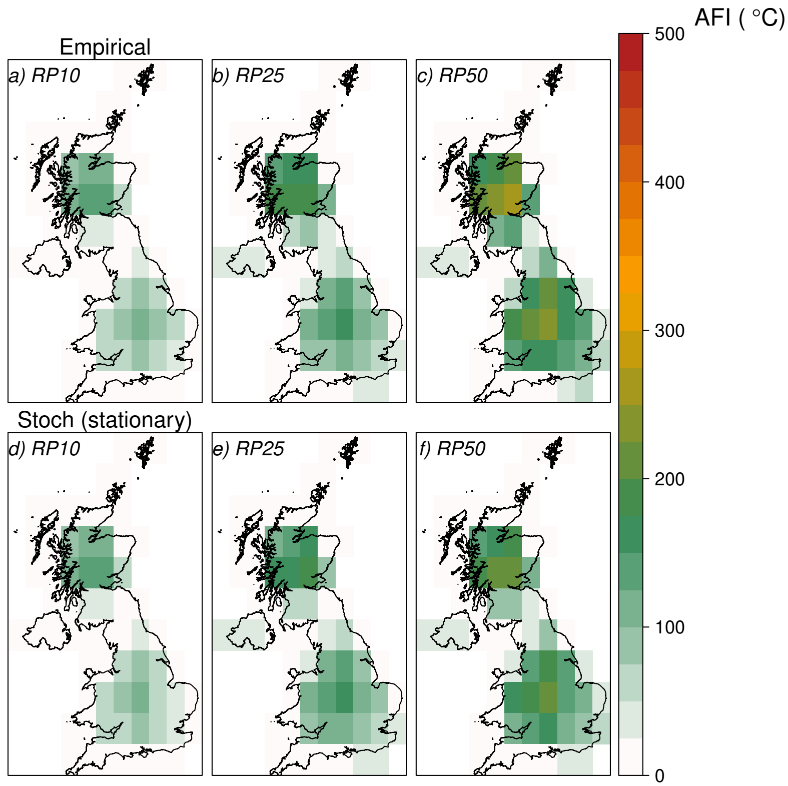
Empirical
a) RP10
b) RP25
c) RP50
Stoch (stationary)
d) RP10
e) RP25
f) RP50
AFI (°C)
500
400
300
200
100
0

predicted for the southern part of UK ~~, as well~~in comparison to the north. The extreme AFI values in the south are ~~again~~ driven by the exceptional 1962/63 winter ~~; exluding~~ which has been more severe in the South than the North (see Fig. 2b). Excluding this winter from the analysis results in almost ~~two times~~ much lower AFI values in most of the region (~~bottom panels in Fig. 5~~not shown).

4.2 Regional return period AFI curves

The vine copula methodology permits the estimation of the hazard return periods over aggregated regions in the UK~~, which is particularly useful for insurance portfolio loss analysis. Results here are shown, apart from the entire UK, for three latitudinal regions: South England, North England & Northern Ireland, and Scotland.~~

. Since our focus is mainly on inhabited areas, for each simulation year (y) and for each region, ~~I compute~~ the "weighted AFI" (wAFI) is computed, where the AFI value at each cell j is weighted by the corresponding number of residential properties (n_j), as shown in Eq. ~~4~~(12). The weighted AFI thus places more weight on the hazard over large populated urban areas than agricultural or ~~mountaineous~~ mountainous areas. The number of residential properties in the UK is taken from the PERILS Industry Exposure Database (https://www.perils.org/), which contains up-to-date high quality insurance market data at Cresta level ("Catastrophe Risk Evaluation and Standardizing Target Accumulations", https://www.cresta.org/) based on data directly collected from insurance companies writing property business in the UK.

$$\cancel{wAFI_{year} = \frac{\sum AFI_{j,year} \cdot n_j}{\sum n_j}}$$

Return period wAFI curves for both the empirical and the stochastic data ~~is~~ are shown in Fig. ~~??. The empirical return~~ 10. Analogous return period plot based on mAFI, i.e. without weighting, can be found in the Appendix (Fig. A1).

$$wAFI_y = \frac{\sum AFI_{j,y} \cdot n_j}{\sum n_j} \tag{12}$$

4.2.1 Model uncertainty

The stationary model is utilized to analyze the uncertainty in the model results and investigate its sources. Fig. 10 shows the empirical and the stochastic return period curves of wAFI for the entire UK, together with their associated uncertainties. The empirical return periods calculation is described in Sect. 4.1, while their uncertainty intervals are computed ~~via~~ from the 2.5^{th} and 97.5^{th} quantile of the beta probability distribution function (**?**). The stochastic curve and confidence intervals are computed as described in Sect. 3.3.2. ~~Analogous return period plots based on the UK average AFI (mAFI), i.e. without weighting, can be found in the Appendix (Fig. A1).~~

4.2.2 ~~The 1962/63 winter return period~~

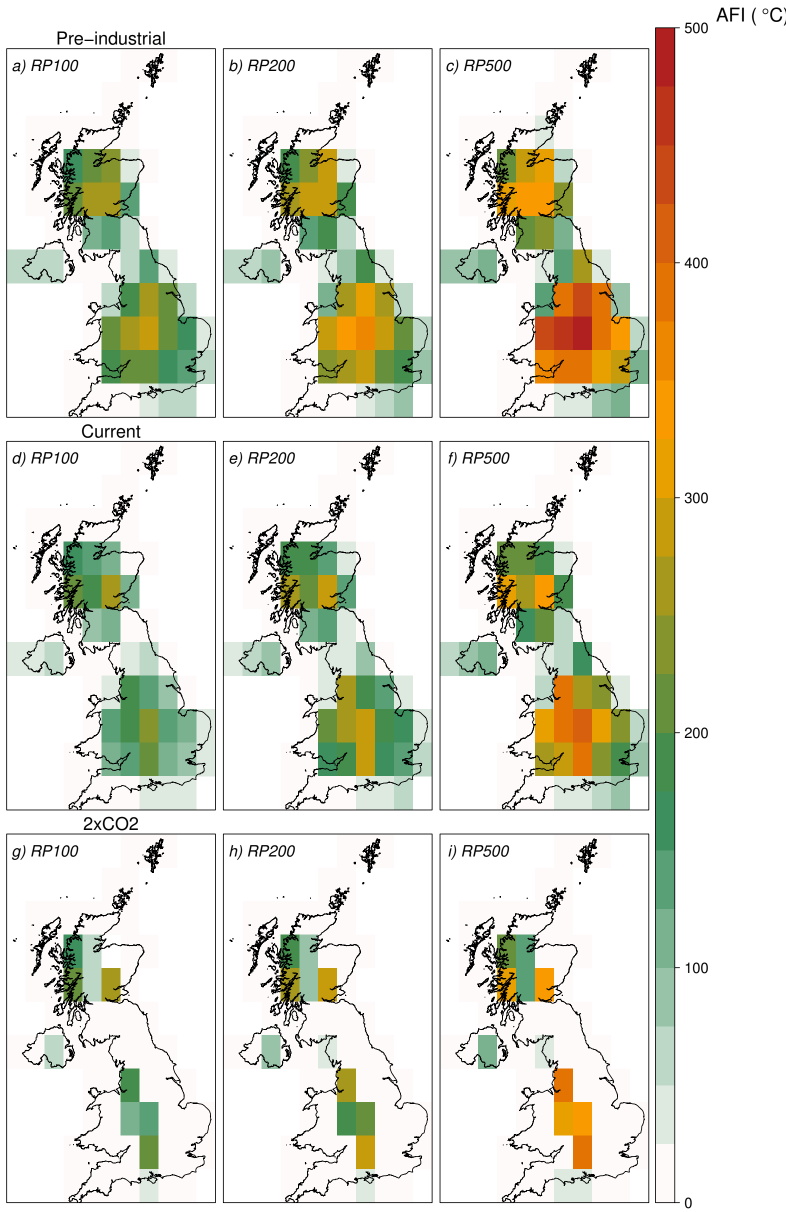

Figure 9. Maps of stochastic AFI values (in °C) for return periods of 1 in 100, 1 in 200, and 1 in 500 years for pre-industrial (top panels), current (middle panels), and 2xCO_2 (bottom panels) climate.

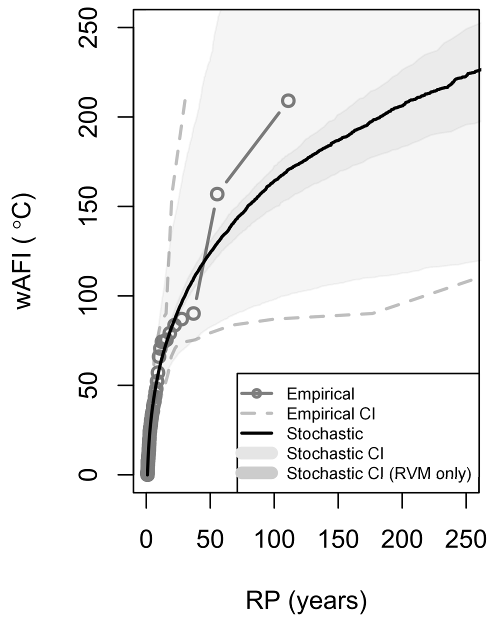

Figure 10. Return period curves of wAFI (in °C) based on the historical data (grey) and the stochastic model (black). The 95% confidence intervals are shown as dashed grey lines for the historical data and as a shaded grey area for the stochastic model. The dark shaded area represents the stochastic uncertainty due to the RVM model alone.

~~The stochastic curve (black line, Fig. ??a) follows closely the empirical one (grey line and circles) apart from the last historical point (with a wAFI of 141C) , which corresponds to~~ The uncertainty in the model is found to be large, only marginally lower, then the empirical estimates and is associated to the short historical record length. Most of the uncertainty (around 90% for RPs greater than 50 years) originates from the uncertainty in the GEV distribution parameters, with the remaining 10% to be due to the RVM model (dark shaded area in Fig. 10). Extreme-value theory is considered as a state-of-the-art procedure to find values for return periods that amply exceed the record length and has been utilized in this study. However, a common difficulty with extremes is that, by definition, data is rare and as a result, the shorter the record length, the more inaccurate is the estimation of the GEV parameters. The results presented in the following sections should therefore be interpreted being aware of the existing uncertainties.

4.2.2 The 1962/63 winter return period and climate change influence

The 1962/63 ~~severe cold winter. This event is estimated empirically as 1 in 52 years event, but with a large uncertainty around this estimate due to the small size of the historical record , as shown by the uncertainy lines in Fig. ??a. In the stochastic set,~~

~~such an extreme winter represents a larger return period of 89 years, with 95% confidence intervals of 81 to 120 years (see table 4). Especially for Southern England (Fig. ??b), this~~ winter has been ~~particularily rare; the model suggests a return period of~~ the coldest in the reanalysis data in the UK and, thus, it is estimated empirically as a 1 in ~~96 (91-138)years, which~~ 110 years event (i.e. the length of the data set). This corresponds well with ~~other independent point measurements. For example, according to~~ the Central England Temperature (CET) record, the oldest continuously running temperature ~~dataset~~ data set in the world (**?**). According to the latter, only two other winters (1683/84 and 1739/40) have been colder than 1962/63 in the last 350 years, suggesting a return period in the range of 110-120 years, as well. The stationary model suggests a longer return period of 205 years for all the UK.

~~Empirical and model return periods in years, including 95% confidence interval ranges in parenthesis, for the 1962/63 winter in the UK. Region Empirical RP (95% CI) Model RP (95% CI) UK89 (81-120) England S. 96 (91-138) England N. & N. Ireland 79 (70-101) Scotland 55 (49-65)~~

~~However, recent studies suggest that cold weather in the UK is likely to be less severe, to occur less frequently, and to last for a shorter period of time than was historically the case due to anthropogenic induced climate change (**?**), although this is still under debate. **?**~~ In particular in the South of the UK the model suggests that this event has been particularly unusual. In the Northern part of UK on the other hand, the model suggests a lower return period of 106 years, closer to the empirical estimate. The non-stationary model suggests that under current climate conditions, such an extreme event, is approximately 2 times less likely to occur than in the 1960s (table 4). This agrees with **?** who used climate model simulations to demonstrate that cold December temperatures in the UK are now half as likely as they were in the 1960s. **?** also indicate that human influence has reduced the probability of such a severe winter in UK by at least 20% and possibly by as much as 4 times, with a best estimate that the probability has been halved. On the other hand, some recent studies have argued that warming in the Arctic could favor the occurrence of cold winter extremes, and might have been also responsible for the unusually cold winters in the UK of 2009/10 and 2010/11 (**??**). This hypothesis though is still largely under debate, see for example **?** and **?**.

~~As shown in Fig. ??b, South England is in general warmer than the North England and Northern Ireland region, partially driven by the urban micro-climate effect of the London area. The~~ Under a $2xCO_2$ climate, a 1962/63 ~~winter was less extreme in this region (wAFI of 139 C) with an estimated~~ is predicted to become almost 10 times more infrequent, having a return period of around 1 in ~~79 years. On the other hand, Scotland is usually significantly colder than the rest of UK, reaching for example AFI values of 100~~ 4000 years. Fig. 11 shows an important reduction in the probability of occurrence of cold extreme events across the whole distribution as a result of the increase of anthropogenic CO_2 concentrations. Larger reductions are found for the most extreme events as well, which is probably related to the large increase of the probability of no negative temperatures (P0) for several cells especially around the coast (see Fig. 9). Similar results are found in both the northern and the southern part of UK, as well (Fig. 11b).

4.2.3 NAO influence

~~The winters 1962/63, 1985/86, 2009/10, 2010/11 were associated with a negative NAO phase (**??**). The NAO has a profound effect on winter climate variability around the Atlantic basin, accounting more than half of the year-to-year variability in~~

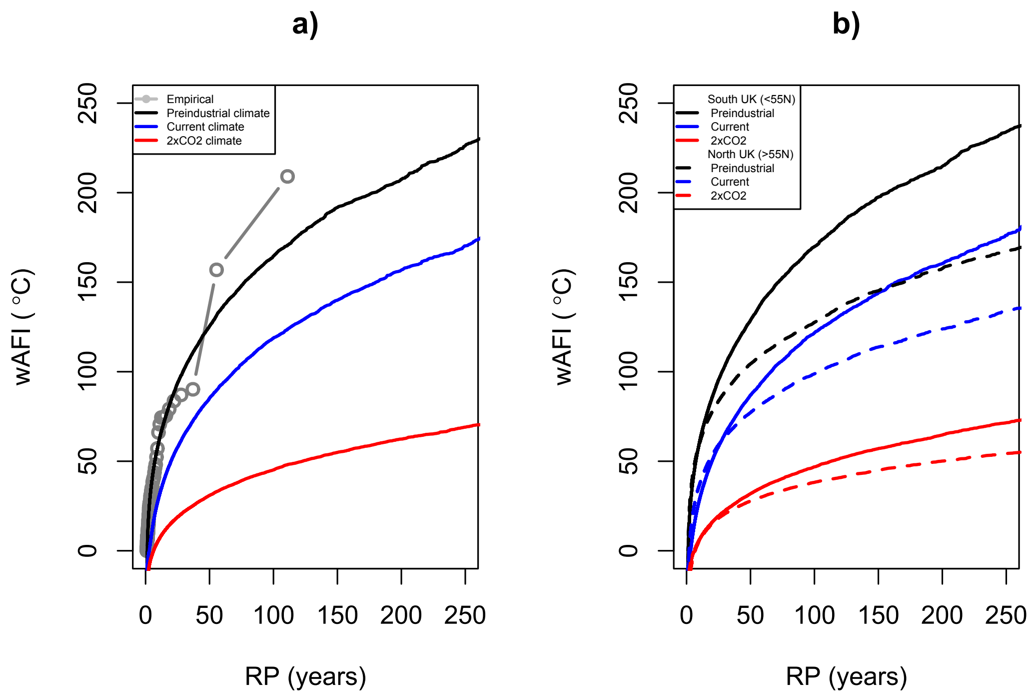

Figure 11. a) Return period curves of wAFI (in °C) based on the historical data (grey) and the stochastic model for three different climate conditions: pre-industrial (black)~~. The 95% confidence intervals are shown as dashed grey lines for the historical data~~ ~~,~~ , current (blue), and ~~as a shaded grey area for the stochastic model~~2xCO_2 (red). ~~The dotted black lines represent the 95% confidence intervals of the stochastic model resulting from the length of the Monte Carlo simulation alone.~~

b) ~~Modelled return period curves of wAFI~~ Same as (~~in C~~a) ~~, for~~ but separated between South ~~England~~ UK (~~red~~full lines) ~~,~~ and North ~~England & Northern Ireland~~ UK (~~green~~dashed lines)~~, and Scotland (blue)~~. ~~The shaded areas denote the respective 95% confidence intervals for each region~~Only stochastic sets are shown.~~The circles specify the winter 1962/63 values on the curves.~~

Table 4. Return period estimates for the 1962/63 winter freeze event, based on wAFI.

Method	All UK	South UK (<55° ~~C almost 2 times more often. However, the curve flattens out shortly after that and more extr~~
Empirical	110	
Stationary stochastic set	205	
Non-stationary stochastic sets		
pre-industrial	204	
1960s	216	
current	433	
$2xCO_2$	4284	

The profound effect of NAO on the winter surface temperature over UK ~~(??). Not surprising, the average AFI over the entire UK is found to be significantly anti-correlated (ρ = -0.59, pval=4.810^{-6}) with the winter (December through March) station-based NAO index (NAOI) (?), as shown in Fig. 2.~~

~~In order to investigate this further, a generalized linear model (GLM) has been introduced into the location parameter of the GEV distributions. More precisely, the location parameter for each cell has been defined as a function of the NAOI: $\mu = \beta_0 + \beta_1 NAOI$ (see Eq. 1 in Sect. 3.3). However, the non-stationary fits were statistically similar to the default model, with β_1 parameters not significantly different from zero. This is probably related to the quite noisy character of the phenomenon and the relatively short historical record used in this study, which makes it difficult to discern the statistical differences in the extreme temperatures between positive and negative NAO winters. The effect of NAO in the hazard dependency structure has not been taken into account here. Recently, **??** developed a methodology that offers the possibility to include such meteorological predictors in~~ has been reported by several studies (**???**). In conjunction with those, the model predicts a negative (positive) NAO phase increases (decreases) substantially the probability of a ~~vine copula model and is something to be addressed in~~ cold event in the UK (Fig. 12). In fact, on average, extreme cold winters are estimated to occur approximately 3 to 4 times more likely during the negative than the positive phase. As an example, an event with wAFI of 100 °C has a ~~future study~~return period of 1 in 39 years, assuming a negative phase, and 1 in 133 years, assuming a positive phase. Because of its intrinsic chaotic behaviour, NAO is difficult (if even possible) to be predicted (**?**). Nevertheless, numerical seasonal forecast systems are currently rapidly improving and have even shown some success in the past (**??**). Incorporating such information in models could be very useful from the catastrophe risk management perspective.

4.2.4 ~~Model uncertainty and sensitivity analysis~~

~~Any modelling results need to be interpreted being aware of their uncertainties. In this study, the main uncertainty in the model and the subsequent return periods stems from four sources: the uncertainty due to the short historical record length the uncertainty resulting from the length of the Monte Carlo simulation (i.e. the number of simulated winters) the uncertainty in~~

~~the joint pdf (i.e. in the RVM) due to the limited historical record the uncertainty due to the model assumption of a stationary climate~~

~~The uncertainty in the historical data is sunbstantial as shown by the dashed grey lines in Fig. **??**a (notice that measurement and interpolation errors in the historical dataset are assumed to be negligible). As an example, the estimated RP 95% confidence interval infor the 1962/63 winter ranges from 14~~ It is important to ~~2015 years. Extreme-value theory is considered as a state-of-the-art procedure to find values for return periods that amply exceed the record length and has been utilized in this study. However, a common difficulty with extremes is that, by definition, data is rare and as a result, the shorter the record length, the more inaccurate is the estimation of the GEV parameters. As a (rather extreme) example, excluding the 1962/63 winter from the analysis would result in a significant reduction of the modelled probability of the occurrence of such an extreme winter to 1 in 831 years. A longer therefore record is needed to reduce this uncertainty. Meteorological reanalysis datasets could provide a comprehensive and consistent gridded temperature dataset over a very long period (e.g. **??**), but higher spatial and temporal resolution is required in order to accurately calculate the air freezing index.~~

~~The dotted black lines in Fig. **??**a show the estimated confidence intervals due to number of years used for the Monte Carlo simulation alone. The obtained uncertainty is important but smaller in comparison to the uncertainty in the empirical curve, i.e. directly from the observed data. Furthermore, the accuracy can be improved by increasing the number of simulated years, but at a computation cost.~~

~~The confidence intervals resulting from the Monte Carlo simulation almost entirely account for the model uncertainty estimated using the parametric bootstrap approach (i.e. which encompasses both (a) and (b) types of uncertainty, see Sect. 3.3.2), suggesting that the uncertainty in the RVM is negligible. As mentioned in Sect. 3.3.1, the reason of the small uncertainy in the RVM is twofold: the large majority of the pairs are estimated to be independent and also the most important dependencies are captured at the first trees. Both reasons lead to a virtual reduction in the dimensions of the pdf. Figure **??**a shows the return period plots for the same RVM but truncated above the first seven levels (i.e. using independent copulas above level 1, 2, 3, up to 7). The same seed as for the default RVM is used in the simulation of these truncated models in order to avoid differences associated with the Monte Carlo sampling. The return period curves are quite similar for the RVMs with truncation above level 2, indicating that the first two levels capture most of the dependency structure~~ note that the effect of NAO in the hazard dependency structure has not been taken into account here. Recently, a methodology that offers the possibility to include such meteorological predictors in a vine copula model has been developed by **??** and is something to be addressed in a future study. Finally, another point that requires further consideration is the mechanisms that control and affect the NAO and its temporal evolution and in particular how the NAO responds to external CO_2 forcing (**?**, e.g.).

~~Another source of uncertainty stems from the fact that the model has been developed under the assumption of a stationary climate, i. e. that the climate has not changed significantly during the last 51 years. Despite the observed winter warming in the UK during the last decades (**?**), its effects in the frequency and magnitude of extreme cold spells is still unclear, as also discussed in Sect. 4.2. To test the non-stationarity assumption, a linear covariate is incorporated in the location parameter of the GEV distributions~~ ~~($\mu = \beta_0 + \beta_1 year$)~~ ~~in order to account for an annual trend in AFI. The resulting~~ ~~β_1~~ ~~parameters were not~~

~~significantly different from zero, indicating an unsubstantial linear trend in AFI during the last five decades. Due to its high year-to-year variability (see Fig. 2), longer monitoring records are needed to identify statistically significant trends.~~

~~Additional sensitivity tests have been performed in order to investigate the influence of selected RVM copula families and parameters to the estimated return periods. Figure **??**b shows the return period curves based on a range of vine copula models that are fitted using subset or single copula families. In comparison to the selected RVM (black line), the choice of a single copula family in the fitting process reduces significantly the co-occurrence of extreme values in the case of Gaussian, Clayton, and Frank copulas. This is to be expected since all those copulas do not show upper tail dependence in the limits. In fact, away from the extremes, the Gaussian copula shows greater upper tail concentration than Frank or Clayton copulas, as also found in the RP results. On the other hand, the copulas that show upper tail dependence (Joe, Gumbel, and Student t), lead to results that are comparable to the default model, which indicates that a selection of a more parsimonious model might be possible. Finally, including the two-parameter Archimedean copulas in the model fitting process (red line in Fig. **??**b) also has minor impact in the estimated return periods in comparison to the default model.~~

5 Conclusions

This paper presents a probabilistic model of extreme cold winters in the United Kingdom. The hazard is modeled using the Air Freezing Index, an index which takes account both the magnitude and the duration of air temperature below freezing and is calculated from ~~temperature data from the last 51 years.~~ the ERA-20C reanalysis temperature data covering the period from 1900 to 2010. Extreme value theory has been applied in order to estimate the probability of extreme cold winters spatially across the UK. More importantly, the spatial dependence between regions in the UK has been assessed through a novel approach which takes advantage of the vine copula methodology. This approach allows the modeling of concurrent high AFI values across the country which is necessary in order to assess reliably the extreme behaviour of such events.

~~A stochastic set of 10K years is generated which is used to estimate the return period~~ Recognizing the non-stationary nature of climate extremes, the model also incorporates NAO and climate change effects as predictors. Stochastic sets of 100K years representing different climate conditions (i.e. pre-industrial, current, or future climate and positive or negative NAO) have been generated and the return periods of extreme cold winters in UK, such as the "Big Freeze of 1962/63" have been estimated. According to the model, such a cold winter is estimated to occur once every ~~89 years in UK, with 95% confidence intervals ranging from 81 to 120 years. Especially for South England, this winter has been particularily rare with a return period equal to 1 in 96 years. It is important to note, though, that~~ approximately 400 years under current climate conditions in the UK. The occurrence of such an event is calculated to have increased approximately two times during the course of the 20th century as a result of anthropogenic climate change. Moreover, the model predicts that such an event will become quite uncommon and occur even more rarely, about 10 times less frequently, under 2xCO_2 climate conditions. The frequency of extreme cold spells in UK has been found to be heavily modulated by NAO, as well. A cold event is estimated to occur ≈3-4 times more likely during the negative than the positive phase.

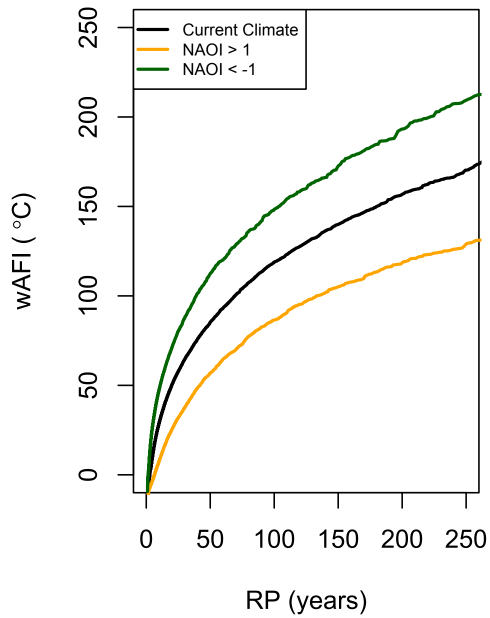

Figure 12. ~~a) wAFI RP~~ Return period curves ~~for~~ of wAFI (in °C) based on the ~~whole UK. The empirical curve is shown~~ current climate stochastic model and assuming a variable NAOI as described in ~~grey. Stochastic results are shown for trucated RVMs above levels 1 to 7~~ the text (~~colored lines) or with no truncation (default,~~ black line). ~~b) Sensitivity tests for the RP~~ Return period curves ~~of wAFI~~ based on ~~RVM fitted using: all available copula families~~ negative (~~black line~~lower than -1) ~~, all but the two-parameter Archimedean copulas~~ and positive (~~i.e. default RVM, red line~~larger than 1) ~~,~~ values of NAOI are shown with green and ~~only one Copula family each time~~orange lines, ~~i~~respectively.~~e. Gaussian (blue line line), Student's t (dashed grey), Clayton (dotted grey line), Gumbel (dotdash grey line), Frank (red line), and Joe (grey line).~~

However, considerable uncertainty exists in these estimates ~~. First and foremost, the 52-year historical~~ which should be interpreted with caution. The 110-year re-analysis record used in this study ~~is~~ has been estimated to be short in order to estimate with enough confidence the frequencies of such extreme events. Additional uncertainty may also be introduced by possible spurious trends in the reanalysis data set. A longer record of temperature data would be necessary in order to reduce the uncertainty and high quality long-term reanalysis products including ensemble approaches could help towards this direction. ~~Additional uncertainty in the model stems from the impacts of our changing climate due to anthropogenic forcing, but further research is necessary in order to discern how exactly extreme winter temperatures are affected in the UK. Singificant improvements are expected to come with increasing availability of data, increasing understanding of the science, and with~~

~~advancements in computing capability and technology. This model is part of a probabilistic catastrophe model for insurance losses due to burst pipes resulting from freezing temperatures.~~

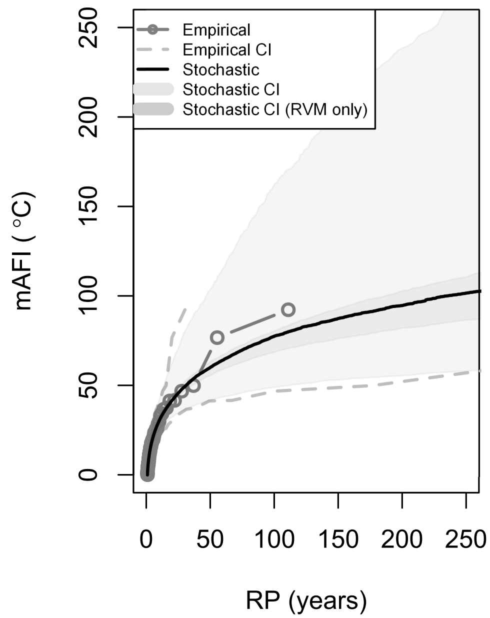

Figure A1. Similar to Fig. ~~??~~ 10 but for mAFI (without weighting, in °C).

Appendix A

A1

Disclaimer. TEXT

Acknowledgements. TEXT

References

Aas, K., Czado, C., Frigessi, A., and Bakken, H.: Pair-copula constructions of multiple dependence,, Tech. rep., Munich University, Institute for Statistics, http://epub.ub.uni-muenchen.de/, 2006.

Abbara, O. and Zevallos, M.: Assessing stock market dependence and contagion, Quantitative Finance, 14, 1627–1641, doi:10.1080/14697688.2013.859390, https://doi.org/10.1080/14697688.2013.859390, 2014.

ABI: Industry Data Downloads, Tech. rep., Association of British Insurers, https://www.abi.org.uk/data-and-resources/industry-data/free-industry-data-downloads/, 2017.

AIR: About Catastrophe Models, Tech. rep., AIR Worldwide, https://www.air-worldwide.com/Publications/Brochures/documents/About-Catastrophe-Models/, 2012.

Barnes, E. A. and Screen, J. A.: The impact of Arctic warming on the midlatitude jet-stream: Can it? Has it? Will it?, Wiley Interdisciplinary Reviews: Climate Change, 6, 277–286, doi:10.1002/wcc.337, http://dx.doi.org/10.1002/wcc.337, 2015.

Bedford, T. and Cooke, R. M.: Vines–a new graphical model for dependent random variables, Ann. Statist., 30, 1031–1068, doi:10.1214/aos/1031689016, https://doi.org/10.1214/aos/1031689016, 2002.

Beguería, S., Angulo-Martínez, M., Vicente-Serrano, S. M., López-Moreno, J. I., and El-Kenawy, A.: Assessing trends in extreme precipitation events intensity and magnitude using non-stationary peaks-over-threshold analysis: a case study in northeast Spain from 1930 to 2006, International Journal of Climatology, 31, 2102–2114, doi:10.1002/joc.2218, https://rmets.onlinelibrary.wiley.com/doi/abs/10.1002/joc.2218, 2011.

Bevacqua, E.: CDVineCopulaConditional: Sampling from Conditional C- and D-Vine Copulas. R package version 0.1.0, R package version 0.1.0, https://cran.r-project.org/web/packages/CDVineCopulaConditional/index.html, 2017b.

Bevacqua, E., Maraun, D., Hobæk Haff, I., Widmann, M., and Vrac, M.: Multivariate statistical modelling of compound events via pair-copula constructions: analysis of floods in Ravenna (Italy), Hydrology and Earth System Sciences, 21, 2701–2723, doi:10.5194/hess-21-2701-2017, https://www.hydrol-earth-syst-sci.net/21/2701/2017/, 2017a.

Bilotta, R., Bell, J. E., Shepherd, E., and Arguez, A.: Calculation and Evaluation of an Air-Freezing Index for the 1981–2010 Climate Normals Period in the Coterminous United States, Journal of Applied Meteorology and Climatology, 54, 69–76, doi:10.1175/JAMC-D-14-0119.1, http://dx.doi.org/10.1175/JAMC-D-14-0119.1, 2015.

Bloomfield, H. C., Shaffrey, L. C., Hodges, K. I., and Vidale, P. L.: A critical assessment of the long-term changes in the wintertime surface Arctic Oscillation and Northern Hemisphere storminess in the ERA20C reanalysis, Environmental Research Letters, 13, 094 004, http://stacks.iop.org/1748-9326/13/i=9/a=094004, 2018.

Bonazzi, A., Cusack, S., Mitas, C., and Jewson, S.: The spatial structure of European wind storms as characterized by bivariate extreme-value Copulas, Natural Hazards and Earth System Sciences, 12, 1769–1782, doi:10.5194/nhess-12-1769-2012, https://www.nat-hazards-earth-syst-sci.net/12/1769/2012/, 2012.

Booth, G.: Winter 1947 in the British Isles, Weather, 62, 61–68, doi:10.1002/wea.66, https://rmets.onlinelibrary.wiley.com/doi/abs/10.1002/wea.66, 2007.

Bowman, G., Coburn, A., and Ruffle, S.: Freeze - Profile of a Macro-Catastrophe Threat Type, Cambridge centre for risk studies working paper series, Cambridge Risk Framework, https://hazdoc.colorado.edu/handle/10590/6787?show=full, 2012.

Brechmann, E. C. and Schepsmeier, U.: Modeling Dependence with C- and D-Vine Copulas: The R Package CDVine, Journal of Statistical Software, doi:10.18637/jss.v052.i03, https://www.jstatsoft.org/article/view/v052i03, 2013.

Cawthorne, R. A. and Marchant, J. H.: The effects of the 1978/79 winter on British bird populations, Bird Study, 27, 163–172, doi:10.1080/00063658009476675, http://dx.doi.org/10.1080/00063658009476675, 1980.

Cheng, L., AghaKouchak, A., Gilleland, E., and Katz, R. W.: Non-stationary extreme value analysis in a changing climate, Climatic Change, 127, 353–369, doi:10.1007/s10584-014-1254-5, https://doi.org/10.1007/s10584-014-1254-5, 2014.

Christidis, N. and Stott, P. A.: Lengthened odds of the cold UK winter of 2010/2011 attributable to human influence [in "Explaining Extreme Events of 2011 from a Climate Perspective"], Bulletin of the American Meteorological Society, 93, 1060–1062, doi:10.1175/BAMS-D-12-00021.1, https://doi.org/10.1175/BAMS-D-12-00021.1, 2012.

Coles, S. G. and Dixon, M. J.: Likelihood-Based Inference for Extreme Value Models, Extremes, 2, 5–23, doi:10.1023/A:1009905222644, https://doi.org/10.1023/A:1009905222644, 1999.

Compo, G. P., Whitaker, J. S., Sardeshmukh, P. D., Matsui, N., Allan, R. J., Yin, X., Gleason, B. E., Vose, R. S., Rutledge, G., Bessemoulin, P., Brönnimann, S., Brunet, M., Crouthamel, R. I., Grant, A. N., Groisman, P. Y., Jones, P. D., Kruk, M. C., Kruger, A. C., Marshall, G. J., Maugeri, M., Mok, H. Y., Nordli, O., Ross, T. F., Trigo, R. M., Wang, X. L., Woodruff, S. D., and Worley, S. J.: The Twentieth Century Reanalysis Project, Quarterly Journal of the Royal Meteorological Society, 137, 1–28, doi:10.1002/qj.776, http://dx.doi.org/10.1002/qj.776, 2011.

Czado, C.: Pair-Copula Constructions of Multivariate Copulas. In: Jaworski P., Durante F., Härdle W., Rychlik T. (eds) Copula Theory and Its Applications. Lecture Notes in Statistics, Springer, doi:https://doi.org/10.1007/978-3-642-12465-5_4, 2010.

Czado, C., E.C.Brechmann, and Gruber, L.: Selection of Vine Copulas. In: Copulae in Mathematical and Quantitative Finance. Lecture Notes in Statistics, Springer, 2013.

D., S. and Schirmacher, E.: Multivariate Dependence Modeling Using Pair-Copulas, Tech. rep., Society of Actuaries., 2008.

Dell'Aquila, A., Corti, S., Weisheimer, A., Hersbach, H., Peubey, C., Poli, P., Berrisford, P., Dee, D., and Simmons, A.: Benchmarking Northern Hemisphere midlatitude atmospheric synoptic variability in centennial reanalysis and numerical simulations, Geophysical Research Letters, 43, 5442–5449, doi:10.1002/2016GL068829, http://dx.doi.org/10.1002/2016GL068829, 2016GL068829, 2016.

Dißmann, J., Brechmann, E., Czado, C., and Kurowicka, D.: Selecting and estimating regular vine copulae and application to financial returns, Computational Statistics & Data Analysis, 59, 52 – 69, doi:https://doi.org/10.1016/j.csda.2012.08.010, http://www.sciencedirect.com/science/article/pii/S0167947312003131, 2013.

Donat, M. G., Alexander, L. V., Herold, N., and Dittus, A. J.: Temperature and precipitation extremes in century-long gridded observations, reanalyses, and atmospheric model simulations, Journal of Geophysical Research: Atmospheres, 121, 11,174–11,189, doi:10.1002/2016JD025480, https://agupubs.onlinelibrary.wiley.com/doi/abs/10.1002/2016JD025480, 2016.

Durante, F. and Sempi, C.: Principles of copula theory, CRC/Chapman & Hall, 2015.

Folland, C. and Anderson, C.: Estimating Changing Extremes Using Empirical Ranking Methods, Journal of Climate, 15, 2954–2960, doi:10.1175/1520-0442(2002)015<2954:ECEUER>2.0.CO;2, 2002.

Folland, C. K., Parker, D. E., Scaife, A. A., Kennedy, J. J., Colman, A. W., Brookshaw, A., Cusack, S., and Huddleston, M. R.: The 2005/06 winter in Europe and the United Kingdom: Part 2 –Prediction techniques and their assessment against observations, Weather, 61, 337–346, doi:10.1256/wea.182.06, http://dx.doi.org/10.1256/wea.182.06, 2006.

Francis, J. A. and Vavrus, S. J.: Evidence linking Arctic amplification to extreme weather in mid-latitudes, Geophysical Research Letters, 39, n/a–n/a, doi:10.1029/2012GL051000, http://dx.doi.org/10.1029/2012GL051000, l06801, 2012.

Frauenfeld, O. W., Zhang, T., and Mccreight, J. L.: Northern Hemisphere freezing/thawing index variations over the twentieth century, International Journal of Climatology, 27, 47–63, doi:10.1002/joc.1372, http://dx.doi.org/10.1002/joc.1372, 2007.

Genest, C. and Favre, A.-C.: Everything You Always Wanted to Know about Copula Modeling but Were Afraid to Ask, Journal of Hydrologic Engineering, 12, 347–368, doi:10.1061/(ASCE)1084-0699(2007)12:4(347), https://ascelibrary.org/doi/abs/10.1061/%28ASCE%291084-0699%282007%2912%3A4%28347%29, 2007.

Gordon, J. R.: An Investigation into Freezing and Bursting Water Pipes in Residential Construction, Research report 96-1, Building Research Council. School of Architecture. College of Fine and Applied Arts. University of Illinois at Urbana-Champaign, http://hdl.handle.net/2142/54757, 1996.

Graham, R. J., Gordon, C., Huddleston, M. R., Davey, M., Norton, W., Colman, A., Scaife, A. A., Brookshaw, A., Ingleby, B., McLean, P., Cusack, S., McCallum, E., Elliott, W., Groves, K., Cotgrove, D., and Robinson, D.: The 2005/06 winter in Europe and the United Kingdom:Part 1 –How the Met Office forecast was produced and communicated, Weather, 61, 327–336, doi:10.1256/wea.181.06, http://dx.doi.org/10.1256/wea.181.06, 2006.

Guirguis, K., Gershunov, A., Schwartz, R., and Bennett, S.: Recent warm and cold daily winter temperature extremes in the Northern Hemisphere, Geophysical Research Letters, 38, n/a–n/a, doi:10.1029/2011GL048762, http://dx.doi.org/10.1029/2011GL048762, l17701, 2011.

Haff, I. H., Frigessi, A., and Maraun, D.: How well do regional climate models simulate the spatial dependence of precipitation? An application of pair-copula constructions, Journal of Geophysical Research: Atmospheres, 120, 2624–2646, doi:10.1002/2014JD022748, https://agupubs.onlinelibrary.wiley.com/doi/abs/10.1002/2014JD022748, 2015.

Hansen, J., Sato, M., Ruedy, R., Kharecha, P., Lacis, A., Miller, R., Nazarenko, L., Lo, K., Schmidt, G. A., Russell, G., Aleinov, I., Bauer, S., Baum, E., Cairns, B., Canuto, V., Chandler, M., Cheng, Y., Cohen, A., Del Genio, A., Faluvegi, G., Fleming, E., Friend, A., Hall, T., Jackman, C., Jonas, J., Kelley, M., Kiang, N. Y., Koch, D., Labow, G., Lerner, J., Menon, S., Novakov, T., Oinas, V., Perlwitz, J., Perlwitz, J., Rind, D., Romanou, A., Schmunk, R., Shindell, D., Stone, P., Sun, S., Streets, D., Tausnev, N., Thresher, D., Unger, N., Yao, M., and Zhang, S.: Dangerous human-made interference with climate: a GISS modelE study, Atmospheric Chemistry and Physics, 7, 2287–2312, doi:10.5194/acp-7-2287-2007, https://www.atmos-chem-phys.net/7/2287/2007/, 2007.

Hurrell, J.: CLIMATE AND CLIMATE CHANGE | Climate Variability: North Atlantic and Arctic Oscillation, in: Encyclopedia of Atmospheric Sciences (Second Edition), edited by North, G. R., Pyle, J., and Zhang, F., pp. 47 – 60, Academic Press, Oxford, second edition edn., doi:https://doi.org/10.1016/B978-0-12-382225-3.00109-2, http://www.sciencedirect.com/science/article/pii/B9780123822253001092, 2015.

Hurrell, J.: The Climate Data Guide: Hurrell North Atlantic Oscillation (NAO) Index (station-based)., Tech. rep., National Center for Atmospheric Research, https://climatedataguide.ucar.edu/climate-data/hurrell-north-atlantic-oscillation-nao-index-station-based, 2017.

Hurrell, J. W.: NAO Index Data provided by the Climate Analysis Section, NCAR, Boulder, USA, Updated regularly. Accessed 12 December 2016, https://climatedataguide.ucar.edu/climate-data/hurrell-north-atlantic-oscillation-nao-index-station-based, 2003.

Hurrell, J. W., Kushnir, Y., Ottersen, G., and Visbeck, M.: An Overview of the North Atlantic Oscillation, pp. 1–35, American Geophysical Union (AGU), doi:10.1029/134GM01, https://agupubs.onlinelibrary.wiley.com/doi/abs/10.1029/134GM01, 2013.

Jenkins, G., Perry, M., and Prior, J.: The climate of the UK and recent trends, Tech. rep., Hadley Centre, Met Office, Exeter, http://ukclimateprojections.metoffice.gov.uk/media.jsp?mediaid=87932&filetype=pdf, 2009.

Joe, H.: Dependence Modeling with Copulas. CRC Monographs on Statistics & Applied Probability., Chapman & Hall, London, 2014.

Katz, R. W., Parlange, M. B., and Naveau, P.: Statistics of extremes in hydrology, Advances in Water Resources, 25, 1287 – 1304, doi:https://doi.org/10.1016/S0309-1708(02)00056-8, http://www.sciencedirect.com/science/article/pii/S0309170802000568, 2002.

Kemp, M.: Tail Weighted Probability Distribution Parameter Estimation, Tech. rep., Nematrian Limited, http://www.nematrian.com/Docs/TailWeightedParameterEstimation.pdf, 2016.

Kushnir, Y., Robinson, W. A., Chang, P., and Robertson, A. W.: The Physical Basis for Predicting Atlantic Sector Seasonal-to-Interannual Climate Variability, Journal of Climate, 19, 5949–5970, doi:10.1175/JCLI3943.1, http://dx.doi.org/10.1175/JCLI3943.1, 2006.

Lee, Y., Shin, Y., and Park, J.-S.: A data-adaptive maximum penalized likelihood estimation for the generalized extreme value distribution, Communications for Statistical Applications and Methods, 24, 493–505, doi:10.5351/CSAM.2017.24.5.493, 2017.

Makkonen, L.: Plotting Positions in Extreme Value Analysis, Journal of Applied Meteorology and Climatology, 45, 334–340, doi:10.1175/JAM2349.1, https://doi.org/10.1175/JAM2349.1, 2006.

Manley, G.: Central England temperatures: Monthly means 1659 to 1973, Quarterly Journal of the Royal Meteorological Society, 100, 389–405, doi:10.1002/qj.49710042511, http://dx.doi.org/10.1002/qj.49710042511, 1974.

Massey, N., Aina, T., Rye, C., Otto, F., Wilson, S., Jones, R., and Allen, M.: Have the odds of warm November temperatures and of cold December temperatures in Central England changed. Bulletin of the American Meteorological Society 93, 1057-1059, Bulletin of the American Meteorological Society, 93, 1057–1059, 2012.

McDonald, A., Bschaden, B., Sullivan, E., and Marsden, R.: Mathematical simulation of the freezing time of water in small diameter pipes, Applied Thermal Engineering, 73, 142 – 153, doi:https://doi.org/10.1016/j.applthermaleng.2014.07.046, http://www.sciencedirect.com/science/article/pii/S135943111400622X, 2014.

Meucci, A.: A Short, Comprehensive, Practical Guide to Copulas, GARP Risk Professional, pp. 22–27, https://ssrn.com/abstract=1847864orhttp://dx.doi.org/10.2139/ssrn.1847864, 2011.

Murray, R.: A note on the large scale features of the 1962/63 winter, Meteorol. Mag., 95, 339–348, 1966.

Myhre, G., Highwood, E. J., Shine, K. P., and Stordal, F.: New estimates of radiative forcing due to well mixed greenhouse gases, Geophysical Research Letters, 25, 2715–2718, doi:10.1029/98GL01908, https://agupubs.onlinelibrary.wiley.com/doi/abs/10.1029/98GL01908, 1998.

Nelsen, R. B.: An Introduction to Copulas, Springer-Verlag, New York., 2006.

on Climate Change", C.: UK Climate Change Risk Assessment 2017. Synthesis report: priorities for the next fi e years, Tech. rep., Committee on Climate Change, https://www.theccc.org.uk/wp-content/uploads/2016/07/UK-CCRA-2017-Launch-slidepack.pdf, 2017.

Osborn, T.: North Atlantic Oscillation, Climatic Research Unit, UEA [WWW document], http://www.cru.uea.ac.uk/cru/info/nao[accessedonFebruary2018], 2000.

Osborn, T. J.: Winter 2009/2010 temperatures and a record-breaking North Atlantic Oscillation index, Weather, 66, 19–21, doi:10.1002/wea.660, http://dx.doi.org/10.1002/wea.660, 2011.

Perry, M. and Hollis, D.: The generation of monthly gridded datasets for a range of climatic variables over the UK, International Journal of Climatology, 25, 1041–1054, doi:10.1002/joc.1161, http://dx.doi.org/10.1002/joc.1161, 2005.

Perry, M., Hollis, D., and Elms, M.: The generation of daily gridded datasets of temperature and rainfall for the UK, Tech. rep., National Climate Information Centre, 2009.

Poli, P., Hersbach, H., Dee, D. P., Berrisford, P., Simmons, A. J., Vitart, F., Laloyaux, P., Tan, D. G. H., Peubey, C., Thépaut, J.-N., Trémolet, Y., Hólm, E. V., Bonavita, M., Isaksen, L., and Fisher, M.: ERA-20C: An Atmospheric Reanalysis of the Twentieth Century, Journal of Climate, 29, 4083–4097, doi:10.1175/JCLI-D-15-0556.1, https://doi.org/10.1175/JCLI-D-15-0556.1, 2016.

Prior, J. and Kendon, M.: The UK winter of 2009/2010 compared with severe winters of the last 100 years, Weather, 66, 4–10, doi:10.1002/wea.735, https://rmets.onlinelibrary.wiley.com/doi/abs/10.1002/wea.735, 2011.

Rind, D., Perlwitz, J., and Lonergan, P.: AO/NAO response to climate change: 1. Respective influences of stratospheric and tropospheric climate changes, Journal of Geophysical Research: Atmospheres, 110, doi:10.1029/2004JD005103, https://agupubs.onlinelibrary.wiley.com/doi/abs/10.1029/2004JD005103, 2005.

Salvadori, G. and Michele, C. D.: On the Use of Copulas in Hydrology: Theory and Practice, Journal of Hydrologic Engineering, 12, 369–380, doi:10.1061/(ASCE)1084-0699(2007)12:4(369), https://ascelibrary.org/doi/abs/10.1061/%28ASCE%291084-0699%282007%2912%3A4%28369%29, 2007.

Salvadori, G., Tomasicchio, G., and D'Alessandro, F.: Practical guidelines for multivariate analysis and design in coastal and off-shore engineering, Coastal Engineering, 88, 1 – 14, doi:https://doi.org/10.1016/j.coastaleng.2014.01.011, http://www.sciencedirect.com/science/article/pii/S0378383914000209, 2014.

Salvadori, G., Durante, F., Tomasicchio, G., and D'Alessandro, F.: Practical guidelines for the multivariate assessment of the structural risk in coastal and off-shore engineering, Coastal Engineering, 95, 77 – 83, doi:https://doi.org/10.1016/j.coastaleng.2014.09.007, http://www.sciencedirect.com/science/article/pii/S0378383914001811, 2015.

Scaife, A. A. and Knight, J. R.: Ensemble simulations of the cold European winter of 2005-2006, Quarterly Journal of the Royal Meteorological Society, 134, 1647–1659, doi:10.1002/qj.312, http://dx.doi.org/10.1002/qj.312, 2008.

Scaife, A. A., Knight, J. R., Vallis, G. K., and Folland, C. K.: A stratospheric influence on the winter NAO and North Atlantic surface climate, Geophysical Research Letters, 32, n/a–n/a, doi:10.1029/2005GL023226, http://dx.doi.org/10.1029/2005GL023226, l18715, 2005.

Schepsmeier, U.: Estimating standard errors and efficient goodness-of- t tests for regular vine copula models, Ph.D. thesis, Fakultat fur Mathematik Technische Universitat Munchen, http://mediatum.ub.tum.de/doc/1175739/document.pdf, 2013.

Schepsmeier, U., Stoeber, J., Brechmann, E. C., Graeler, B., Nagler, T., and Erhardt, T.: VineCopula-package: Statistical Inference of Vine Copulas, Tech. rep., R package, https://cran.r-project.org/web/packages/VineCopula/VineCopula.pdf, 2017.

Seager, R., Kushnir, Y., Nakamura, J., Ting, M., and Naik, N.: Northern Hemisphere winter snow anomalies: ENSO, NAO and the winter of 2009/10, Geophysical Research Letters, 37, n/a–n/a, doi:10.1029/2010GL043830, http://dx.doi.org/10.1029/2010GL043830, l14703, 2010.

Sklar, A.: Fonctions de répartition à n dimensions et leurs marges, Publications de l'Institut de Statistique de L'Université de Paris, 8, 229–231, 1959.

Tang, Q., Zhang, X., Yang, X., and Francis, J. A.: Cold winter extremes in northern continents linked to Arctic sea ice loss, Environmental Research Letters, 8, 014 036, http://stacks.iop.org/1748-9326/8/i=1/a=014036, 2013.

Wallace, J. M., Held, I. M., Thompson, D. W. J., Trenberth, K. E., and Walsh, J. E.: Global Warming and Winter Weather, Science, 343, 729–730, doi:10.1126/science.343.6172.729, http://science.sciencemag.org/content/343/6172/729, 2014.

Walsh, J. E., Phillips, A. S., Portis, D. H., and Chapman, W. L.: Extreme Cold Outbreaks in the United States and Europe, 1948–99, Journal of Climate, 14, 2642–2658, doi:10.1175/1520-0442(2001)014<2642:ECOITU>2.0.CO;2, 2001.

Woollings, T., Hannachi, A., Hoskins, B., and Turner, A.: A Regime View of the North Atlantic Oscillation and Its Response to Anthropogenic Forcing, Journal of Climate, 23, 1291–1307, doi:10.1175/2009JCLI3087.1, https://doi.org/10.1175/2009JCLI3087.1, 2010.